INSTRUMENTS AND METHODS OF INVESTIGATION

PACS numbers: **42.62.–b,** 42.68.Wt, **52.77.–j**

40th ANNIVERSARY OF THE PROKHOROV GENERAL PHYSICS INSTITUTE, RUSSIAN ACADEMY OF SCIENCES

Modern physical methods and technologies in agriculture

S V Gudkov, R M Sarimov, M E Astashev, R Yu Pishchalnikov, D V Yanykin, A V Simakin, A V Shkirin, D A Serov, E M Konchekov, N G Gusein-zade, V N Lednev, M Ya Grishin, P A Sdvizhenskii, S M Pershin, A F Bunkin, M Kh Ashurov, A G Aksenov, N O Chilingaryan, I G Smirnov, D Yu Pavkin, D O Hort, M N Moskovskiy, A V Sibirev, Ya P Lobachevsky, A S Dorokhov, A Yu Izmailov

DOI: https://doi.org/10.3367/UFNe.2023.09.039577

Contents

S V Gudkov [1,2,a], **R M Sarimov** [1,b], **M E Astashev** [1,c], **R Yu Pishchalnikov** [1,d], **D V Yanykin** [1,e], **A V Simakin** [1,f], **A V Shkirin** [1,g], **D A Serov** [1,h], **E M Konchekov** [1,i], **N G Gusein-zade** [1,j], **V N Lednev** [1,k], **M Ya Grishin** [1,l], **P A Sdvizhenskii** [1,m], **S M Pershin** [1,n], **A F Bunkin** [1,o], **M Kh Ashurov** [1,3,p], **A G Aksenov** [2,q], **N O Chilingaryan** [2,r], **I G Smirnov** [2,s], **D Yu Pavkin** [2,t], **D O Hort** [2,u], **M N Moskovskiy** [2,v], **A V Sibirev** [2,w], **Ya P Lobachevsky** [2,x], **A S Dorokhov** [2,y], **A Yu Izmailov** [2,z]

[1] Prokhorov General Physics Institute, Russian Academy of Sciences, ul. Vavilova 38, 119991 Moscow, Russian Federation
[2] Federal Scientific Agroengineering Center VIM, 1st Institutskii pr. 5, 109428 Moscow, Russian Federation
[3] Institute of Nuclear Physics, Academy of Sciences of the Republic of Uzbekistan, pos. Ulugbek, 100214 Tashkent, Uzbekistan

E-mail: [a] S_makariy@rambler.ru, [b] rusa@kapella.gpi.ru, [c] Astashev@yandex.ru, [d] rpishchal@kapella.gpi.ru, [e] ya-d-ozh@rambler.ru, [f] avsimakin@gmail.com, [g] AVShkirin@mephi.ru, [h] dmitriy_serov_91@mail.ru, [i] eukmek@gmail.com, [j] namik@fpl.gpi.ru, [k] lednev@kapella.gpi.ru, [l] mikhail.grishin@phystech.edu, [m] pausdw@gmail.com, [n] pershin@kapella.gpi.ru, [o] abunkin@kapella.gpi.ru, [p] ashurov49@mail.ru, [q] 1053vim@mail.ru, [r] narek-s@list.ru, [s] rashn-smirnov@yandex.ru, [t] dimqaqa@mail.ru, [u] dmitriyhort@mail.ru, [v] maxmoskovsky74@yandex.ru, [w] sibirev2011@yandex.ru, [x] lobachevsky@yandex.ru, [y] dorokhov@rgau-msha.ru, [z] vim@vim.ru

Received 10 August 2023, revised 25 September 2023
Uspekhi Fizicheskikh Nauk **194** (2) 208 – 226 (2024)
Translated by Yu V Morozov

Abstract. **The review presents both new theoretical and practical results of the application of modern physical methods and technologies in agriculture. Physical technologies and materials for passive management of the solar spectrum in greenhouses are considered. A review of the instrumentation used for laser remote sensing of agro- and biosystems and modern laser express technologies used for express analysis of the chemical composition of a substance is carried out. Optical methods used in biological and agricultural diagnostics, including methods based on Mueller polarimetry, are described in detail. A separate chapter of the review is devoted to the production and application of nano-sized objects in agriculture and the food industry. The use of numerous plasma technologies in agriculture is considered.**

Keywords: physical technologies, agriculture, nanoparticles, photoconversion materials, hyperspectral imaging, lidar, spectroscopy, plasma, composite materials

1. Introduction

Obviously, the sustainable environmental development of human society, first and foremost in the agricultural sector and the processing industry, is impossible without the introduction of new methods and technologies. The purpose of this review is to objectively estimate the nature of implementation and application of physical methods available for the solution to agricultural problems. The review is designed to report and discuss both new theoretical and practical results obtained in this area. Physical technologies and materials for the passive control of the solar spectrum in greenhouses, devices for the laser-assisted remote sensing of agricultural and biological systems, and modern laser express technologies for chemical analysis are considered. Optical methods used in biological and agricultural diagnostics — including those based on Mueller polarimetry — are described in detail. A separate chapter of the review is devoted to the production and application of nano-sized objects in agriculture and the food industry. The use of numerous plasma technologies in agriculture is overviewed.

2. Theoretical analysis of the optical properties of photosynthetic pigments and proteins using evolutionary optimization algorithms

Photosynthesis is a light-controlled process leading to the formation of organic compounds from carbon dioxide and water. The intensity of photosynthesis depends on the efficiency of interaction of plant pigments with light quanta. Interpretation and analysis of experimental data available from the optical spectroscopy of organic molecules and crystals in terms of modern semi-classical quantum theories are much more complicated [1, 2] than the study of the optical properties of inorganic pigments and requires powerful computational resources. A main feature of organic pigments consisting of tens and hundreds of atoms is the absence of perfectly symmetric atomic configurations, which hampers simplification of theoretical calculations. The same applies to organic crystals and photosynthetic pigment-protein complexes. In fact, the only solution to the problem is to build up approximate quantum models of varying degrees of complexity and conduct exclusively numerical simulations. However, such an approach leads to the ambiguity of the results obtained, difficulty in estimating their statistical significance, and the necessity to provide evidence of the unique character of the found models of the physical processes under study.

The current development of computer technologies and related dataprocessing and modeling methods has made it possible to bring up such an area of applied mathematics as the modeling of physical and chemical processes in proteins to a fundamentally new level. A key role was played by the development of genetic optimization algorithms designed to minimize multiparameter multimodal functions [3, 4]. The main feature of this algorithm is the use and formalization of such ideas and concepts of natural selection as population, generation, mutation, and crossing. As far as the study of primary processes of photosynthesis is concerned, the genetic algorithms have already been used to simulate energy transfer in photosystem I from the main antenna to the reaction center [5–7], to characterize electronic excited states of chlorophyll in the reaction center of photosystem II [8], and to simulate energy transfer in the LHCII light-harvesting complex [9] and the Fenna–Matthews–Olsen antenna complex of green sulfur bacteria [10]. The main disadvantage of this algorithm is that the parameters of the minimized function are varied discreetly, which causes poor convergence, and as a result, the algorithm was applied only to a limited extent.

Most of the drawbacks of genetic algorithms were eliminated in the so-called evolutionary heuristic optimization algorithms [11–13]. A key feature of these methods is their primary focus on the way the parameters are mutated rather than population diversity. No restrictions (smoothness, continuity) are imposed on the minimized function. Importantly, the values of the optimized parameters change continuously rather than being selected in a discrete manner, as in a genetic algorithm. One of the widely used algorithms of this type is differential evolution [14, 15]. The use of this method for modeling the optical response of photosynthetic pigments and proteins was investigated in detail in the following series of studies [16–20]. The spectra were fitted using special software including both procedures for the differential evolution algorithm and those for the calculation of the linear optical response (Fig. 1).

Modeling the absorption spectra of monomeric molecules in solvents was carried out within the framework of the theory of multimode Brownian oscillators [21]. This semiclassical theory allows us to calculate the absorption line profile of the electronic transition of any organic pigment without resorting to costly *ab initio* quantum calculations. The key element of this theory is the spectral density function describing the interaction of the electronic state with the effective vibrational modes of the molecule. The number of vibrational modes as well as the intensity of their interaction with the electronic transition for each molecule being highly specific, the spectral density can be considered as a unique identifier of electronic transitions in the molecule.

In the case of calculations of the optical response of a system of interacting pigments such as chlorophyll and pheophytin molecules in the reaction center of photosystem II or photosystem I [5, 6, 8, 17, 20], the resulting spectrum can not be considered simply to be the sum of the contributions of each pigment. To model individual contributions of electronic transitions of each molecule, it is necessary to use the exciton theory [1, 2, 21], in the context of which a numerical solution to the Liouville–von Neumann equation for the density matrix is sought [22]. Depending on the spatial arrangement of the pigments in the system and the intensity of interaction of electronic excitations with the vibrational modes and the immediate protein environment, different methods for calculating the relaxation tensor can be used [21].

Summarizing the above, it should be noted that the coordinated performance of the optimization algorithm and optical response procedures requires preliminary configuration and testing. To achieve an optimal operation regime, it is necessary to choose an appropriate strategy for calculating mutant vectors and set such parameters of differential evolution (F — the weighting coefficient, Cr — the crossover probability) that ensure the maximum speed of convergence [17, 19].

The described methodology enables to simulate the optical response of pigment-protein complexes present in the thylakoid membrane of higher plants and evaluate the efficiency of energy exchange between complexes in case of potential modification of the protein matrix and or changes in the spatial arrangement of pigments, which is necessary in molecular biological work aimed at increasing the efficiency of agricultural systems.

3. Physical technologies and materials for the passive management of the solar spectrum in greenhouses

Clearly, the efficiency of an agricultural system can be improved not only by the breeding of plants with chimeric or mutant pigment-protein complexes. An alternative approach is to search for a light source optimal in terms of duration, intensity, and spectral composition. At different times, numerous of approaches have been proposed or

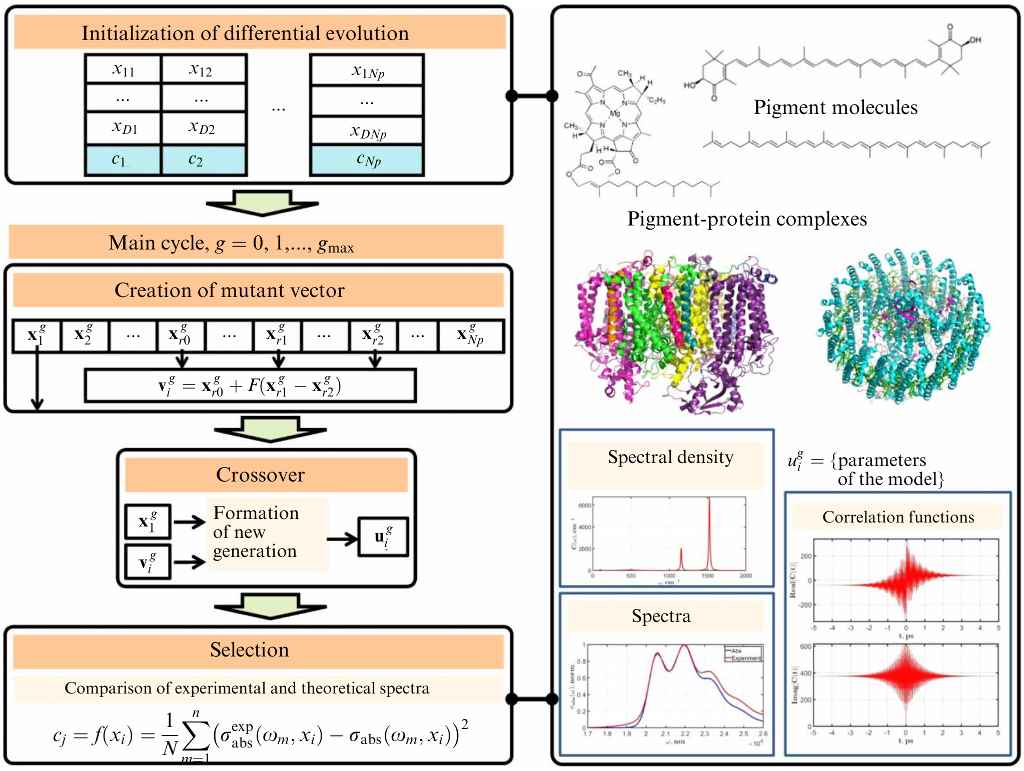

Figure 1. Block diagram of the algorithm for modeling absorption spectra of pigments and photosynthetic pigment-protein complexes. Left: visualization of the differential evolution: initial stage is initialization, then the main cycle of work that includes the functions of calculating the mutant vector, crossover, and selection. Chemical structures of studied pigments and pigment-protein complexes are shown on the right: chlorophyll A, carotenoids, and reaction center of photosystem II and LH1 complexes of purple bacteria. Bottom right: three procedures necessary to calculate absorption spectra within the framework of the theory of multimode Brownian oscillators. See [16, 19] for a detailed description of the operation of this optimization scheme.

implemented to improve insolation that can be conditionally combined into several groups. The first one includes methods aimed at increasing the overall maximum speed of light falling on plants or the so-called flux density of photosynthetically active radiation (PAR). The simplest, but most expensive, method is additional illumination using a variety of light sources, from incandescent lamps to LEDs [23–26]. The second group combines approaches aimed at changing the spectrum of sunlight. Artificially changing the solar spectrum without increasing its intensity (sometimes even with its decrease) may be advisable, because it is known that plants use solar radiation of different wavelengths with different efficiency [27]. Ultraviolet radiation (315–400 nm) can negatively affect the growth and development of plants. A number of studies have demonstrated the positive effect of reducing ultraviolet radiation on plants [28]. Green light (500–565 nm) is very poorly absorbed by the photosynthetic apparatus of plants and its absence, according to some data, has virtually no effect on plants [29]. Far-red light (700–800 nm) is likewise not directly used in photosynthesis [30]. The effect of ultraviolet, green, and far-red light as a rule comes down to the regulation of biochemical and physiological processes in plants due to a change in the proportion of such radiation in the overall spectrum. For this purpose, plants have developed receptor systems [31]. Photosynthesis occurs most efficiently under red (600–700 nm) and blue (440–500 nm) radiation, i.e., in the range of maximum light absorption by pigments of photosynthetic antenna complexes [32]. Moreover, under conditions of insufficient illumination, it is blue and red light that most effectively intensify photosynthesis and, consequently, the growth and development of plants, thus ensuring the maximum yield of agricultural plants [33].

Without the use of artificial lighting sources, changes in the solar spectrum under greenhouse conditions can be achieved in two ways: using either photoselective or photoconversion coatings. The former is based either on reducing the intensity of the spectral component harmful to plants to minimize the damage caused by such light or on changing the ratio of spectral components in order to influence the plants' receptor regulatory systems to increase their productivity as well as the formation of the desired phenotype. The second method involves selective absorption of light by phosphors and re-emission in a different spectral range [34].

The principle of operation of photoselective coatings is based on the selective absorption of light in a certain spectral range owing to dyes inserted in them. Most often, these dyes absorb UV, red, or far-red radiation, and less often blue light [35, 36]. For example, changing the ratio of the proportion of red light to the proportion of far-red light has a great influence on the growth and development of plants [37, 38]. At the dawn of application of photoselective coatings, a copper sulfate solution was widely used as a dye, since it reduces the intensity of far-red light, helping to regulate plant height and the number and size of leaves [39, 40]. Despite their effectiveness, such coatings have a number of disadvantages that limit their use for crop production. They include high cost, the difficulty of maintenance, and phytotoxicity. As an alternative, photoselective coatings based on organic dyes have been developed to absorb light more selectively. As a rule, researchers do not indicate the composition of these dyes in their publications, referring to trade secrets. Among the advantages of using organic dyes is their wide variety, which allows selecting (and combining) them for illumination control in a given part of the solar spectrum. Other undeniable advantages of organic dyes are ease of use, the simplicity of the dye manufacturing process, and their introduction into greenhouse coatings. It is worth noting, however, that such coatings are more in demand for the growth of ornamental plants of profitable presentation than for the cultivation of agricultural crops.

It is known that the share of photons in the blue and red parts of the spectrum among the total number of photons reaching Earth's surface does not exceed 30% [41]. This means that most of the solar energy can potentially be used without a loss of lighting quality [42]. For example, technologies are being developed to convert the energy of UV, green, or far-red photons into electrical [43] or thermal [44, 45] energy, as well as into red and blue photons [46–48]. The electrical and thermal energy can be used for the maintenance of the greenhouse itself, while the absorption of photons with certain characteristics and the emission of those with different properties (photoconversion) can qualitatively change the solar spectrum by increasing PAR density and simultaneously decreasing the spectrum component harmful to plants.

The use of photoconversion coatings separately or in combination with artificial lighting can significantly reduce energy costs and increase crop yields. In order for a photoconversion coating to be effective, it must satisfy the following requirements: the maximum transmission of sunlight effectively used by plants during photosynthesis, the maximum absorption of light in the target ranges, a high quantum yield of luminescence, and minimal reabsorption losses, as well as high chemical and photostability of phosphors. In practice, it is very difficult to produce materials that meet all these requirements, but photoconversion coatings are being improved every year [49].

Phosphors used in photoconversion coatings can be divided into those based on organic dyes [50–52] and those based on metal-containing nanoparticles [53, 54]. Currently, the most common phosphors are based on organic dyes, since they are readily integrated into the coating and, compared to other types of phosphors, have a low cost. However, coatings containing organic dyes quickly fade and lose effectiveness [55]. Phosphors based on rare earth metals and their compounds (e.g., europium) show enhanced stability but low luminescence quantum yield [56]. Quantum dots (cadmium–selenium, zinc–sulfur, etc.) are poorly integrated into polymer matrices and are highly sensitive to reactive oxygen species formed during phosphor functioning [57–59].

It has been mentioned above that plant growth and development are most effectively stimulated by red and blue light, with the efficiency of red photons being significantly higher than that of blue ones. For this reason, roughly 2/3 of photoconversion coatings contain phosphors that convert the absorbed light into the red one. Fifteen percent of publications report the conversion of the absorbed light to blue. At the same time, photoconversion coatings widely used in greenhouses absorb light in those parts of the solar spectrum that are poorly used by plants in the process of photosynthesis (UV, green, and far-red light).

Most often, photoconversion coatings are used to increase the productivity of agricultural crops, such as tomatoes, lettuce, cucumbers, cabbage, and peppers. Less commonly, such coatings are used to grow ornamental plants [60], because photoconversion coatings qualitatively and directionally change the solar spectrum. The main disadvantage of photoconversion coatings remains the relative complexity of manufacturing phosphors, which often leads to an increase in their cost. At the same time, methods for producing photoconversion nanoparticles are constantly being optimized, and experts expect them to become a universal alternative means for increasing crop yields in the near future [61].

Most phosphors in photoconversion coatings act as Stokes emitters liberating a photon with a lower energy than the absorbed one. Some phosphors are capable of emitting photons with higher energy than those used for excitation; they are called upconversion phosphors. The use of upconversion phosphors in greenhouse coatings may have good prospects due to the fact that sunlight contains a large amount of low-energy radiation that is barely used by plants. Such phosphors were proposed in the middle of the 20th century [62]. Recently, several successful applications of upconversion phosphors of the nominal composition $Sr_{0.46}Ba_{0.50}Yb_{0.02}Er_{0.02}F_{2.04}$ [63], $Sr_{0.910}Yb_{0.075}Er_{0.015}F_{2.090}$, [64] and $Sr_{0.955}Yb_{0.020}Er_{0.025}F_{2.045}$ [65] have been demonstrated as glass for greenhouse coatings. In tomato plants (*Solatium lycopersicum*) growing under such coverings, the number and area of leaves, stem length, and chlorophyll content tend to increase. It was found that, in these plants, the functioning of the photosynthetic apparatus in response to the appearance of a violet component in growth illumination is significantly less disrupted, and the restoration of parameters occurs much faster (by about 20–25%).

To improve the efficiency of greenhouse systems equipped with photoconversion materials, modifications to lighting and photoconversion systems have been proposed. Ertürk's modification involves the use of a Lambertian fluorescent reflector [66], which increases the number of converted photons. The principle of its operation consists in light being collected by parabolic collectors equipped with sun tracking systems. The light from the collectors is supplied through a light distribution system (fiber optics, lenses, splitters) to racks with plants. An optical fiber coming from the bottom of the rack is directed to a fluorescent reflector in the ceiling which evenly distributes the light. The fluorescent reflector consists of photoconversion glass containing the fluorescent dye $K_2SiF_6:Mn^{4+}$ that converts ultraviolet and blue-green light (from 300 nm to 520 nm) into red (with maxima at 615 nm, 630 nm, and 650 nm) and a Lambertian reflector. It should be noted that the Lambertian reflector in the fluorescent coating increases the possibility of re-absorption of light by fluorescent pigments by increasing the path length of the light flux [67]. Results of Monte Carlo numerical simulation predict a 35% increase in lettuce (*Lactuca sativa*) yield using the above system.

An interesting modification of greenhouse lighting systems was developed by Makarov and co-workers. They proposed hubs with fiber optic communications [68]. This system allows illuminating the lower leaves of plants shaded by the upper ones. The system consists of a concentrator filled with a phosphor. $CuInSe_xS_{2-x}/ZnS$ quantum dots and an optical fiber through which light is transmitted were used in Ref. [68]. The effectiveness of the described system was demonstrated on tomato plants, the yield of which increased by 7% compared with the control group. The authors attribute the success of their system to both a rise in the total amount of photosynthetically active radiation and more uniform illumination of the plants. It is known that under low-intensity lighting conditions an increase in PAR by 1% increases the yield by up to 1% [69]. Despite some serious shortcomings (low efficiency of light transfer due to surface losses in the concentrator and optical fiber), the system shows good results, which makes promising its further modernization. Surface losses are a key factor in luminescent solar concentrators, and numerous attempts have been made in recent decades to minimize them through homeotropic alignment of phosphors [70] and the use of selective mirrors for light polarization [71]. Losses in optical fibers are reduced by using rough surfaces, materials with different refractive indices, and various micro- or nanostructures [72].

The existing methods of light conversion can significantly increase productivity and improve the morphological characteristics of most plants. However, the choice and application of concrete technologies depend on climatic and seasonal conditions, not to mention the needs of the plants being grown.

4. Laser remote sensing in agriculture

Modern high-tech and highly efficient farming requires continuous monitoring of numerous parameters characterizing the agricultural production process, from the analysis of soil quality to the assessment of the plant growth rate [73]. Continuous monitoring of the state and development of plants under greenhouse conditions can be implemented using a variety of sensors. However, the bulk of agricultural plants are grown in open ground over large areas [74], which makes it difficult to create continuous monitoring systems using sensors. Monitoring large areas is possible only by remote sensing methods, including measurements from satellites and aircraft [75, 76]. These approaches are based on passive sensing methods, such as high-resolution photometry of the areas of interest in various ranges of the optical spectrum [77]. One of the main disadvantages of this approach is its strong dependence on external conditions: the spectral parameters of sunlight vary significantly depending on the concentration and nature of atmospheric aerosols, the presence of fog, geographic latitude, and the time of measurement. Taken together, all these factors require calibration of cameras and sensors immediately before and after the measurements, which reduces the prospects for complete automation of such work and makes it difficult to compare the results obtained by different groups of researchers in different geographical areas.

An alternative approach free from these drawbacks is a laser remote sensing [78]. Active sensing using Lidar (Light Detection And Ranging) — the "detection and measurement of distances using light" — provides advantages over passive sensing by multispectral imaging methods; with this approach, there is no need for precise calibration of the device: one can work day and night since there is no strong influence of sunlight. The use of synchronous detection techniques makes it possible to isolate very weak signals. The first publications reporting the development of lidar were focused on sensing air and water environments. Studies that appeared in the 1980s–1990s focused on diagnosing the state of forests by laser remote sensing [79]. Systematic studies of the possibilities of laser sensing of forests were carried out within the framework of the Laserfleur project (LASFLEUR) in which a team of European scientists developed lidar to record fluorescence spectra and used the data obtained to estimate the general condition of a plant and elucidate the cause of stress, if any [80, 81]. However, such lidar devices were heavy (> 130 kg) and energy-intensive (> 1500 W). Simultaneously, a series of lidar devices was developed at the Institute of General Physics, USSR Academy of Sciences, for analyzing the ocean from an aircraft [82, 83]. Those instruments were also used for sensing vegetation over the land surface. They failed to be employed in agriculture in the 1990s for three reasons, viz. the high cost of lidar instruments themselves, the high cost of air transport, and the lack of free access to the global positioning system (later, its low accuracy) [84]. In the 2000s, compact custom receivers for the global positioning system became available, and significant progress was made in the development of compact and efficient laser sources and optical radiation detecting systems. The situation changed dramatically in the 2010s, when small and cost-effective unmanned aircraft appeared due to the advent of lightweight, energy-intensive, and high-current lithium batteries, as well as affordable high-speed microcontrollers that support the rotation of the devices' numerous motors [85]. The drones development has stimulated the use of compact color, multi-, and hyperspectral cameras mounted on them to monitor agricultural crop areas. However, a similar amount of work has not been done as regards the use of lidar because of technical difficulties arising from limitations imposed on the mass and energy consumption of the devices transported by modern small-size ($20 \times 20 \times 20$ cm^3), low-power (less than 30 W), and low-weight (less than 2–3 kg) modern unmanned aircraft (copters). Only in the last few years have the first publications appeared where the development of fluorescent lidar for monitoring in agriculture and environmental control is described [86–89].

Two research groups have developed truly compact lidar instruments for unmanned aircraft. The most compact fluorescent lidar device was proposed by the Institute of General Physics of the Russian Academy of Sciences for diagnosing the state of plants in the urban environment (operational environmental monitoring) and on agricultural grounds (transition to precision agriculture) [90]. Figure 2 presents the compact fluorescent lidar instrument weighing 310 g and photographs taken during measurements from a drone. This device made it possible to discover areas of a field where plants experience the greatest stress. An additional application of this device included the development of an approach for the rapid measurement of silage moisture that can be useful for high-efficiency livestock production [91].

Also, a compact lidar device was developed at the South China Normal University. It has a greater sensing range and, accordingly, is rather heavy (3.2 kg) [92]. It was used for express environmental monitoring of the surface of fresh water bodies and for the assessment of the condition of trees in the urban environment.

One of the most promising applications of laser spectroscopy and laser physics for addressing practical problems in agriculture is the development of lidar instruments for remote sensing. A combination of low-cost exploitation of unmanned aircraft and further progress in laser technologies makes it possible to develop compact lidar devices for sensing from a distance of a few meters, which is sufficient for mapping crop fields and assessing the environmental situation. The use of fluorescent lidar devices provides information on the state of plants, including the dynamics of their

Figure 2. (a) Schematic of a compact fluorescent lidar instrument. (b) Photograph of a fluorescent lidar device mounted on a drone. (c) Photograph of the process of measuring a corn field from a drone equipped with a fluorescent lidar device.

development cycle, which is another tool for the transition to precision agriculture. For the wide application of lidar in agriculture, further miniaturization and reduction in energy consumption are necessary based on further progress in laser technologies and improvement in detectors.

5. Laser induced breakdown spectrometry for rapid chemical analysis in agriculture

The high rate of urbanization and rapid population growth have a significant negative impact on the environment and the agricultural sector. Human economic activity leads to environmental pollution. For example, water and soil are contaminated with heavy metals that can not only reduce crop yields but also enter the body of domestic animals with plant food and accumulate in dangerous concentrations [93], posing a serious threat to humans, the final consumers of agricultural products. The detection of heavy metals in human and animal foods is an important task for the responsible farmer or producer of high-quality food products. Modern analytical methods for determining the elemental chemical composition, such as atomic absorption spectroscopy, atomic emission spectroscopy, and mass spectroscopy, meet all the requirements for the analysis of soil, water, vegetation, and food. However, they require expensive equipment and highly qualified specialists as well as significant time and labor costs for sample preparation and carrying out analytical procedures [94]. A modern agricultural enterprise needs devices that do not require highly qualified personnel to operate them with a good reliable result and, ideally, making measurements possible directly in the field or on-line control over the production line. A good option for solving these problems is the use of portable devices based on the principles of X-ray fluorescence spectrometry [95] and laser induced breakdown spectrometry (LIBS) [96]. The former has been widely used in practice for more than ten years. It takes several minutes to perform one measurement but requires special protection from X-ray radiation, which is difficult to achieve with a large volume of work carried out by unqualified personnel. In the last decade, increasing interest in applied chemical analysis has been given to the LIBS method, which has a number of advantages, such as a high speed (several seconds), no danger of damage from X-ray radiation, the possibility of simultaneous determination of heavy and light elements, and remote analysis.

LIBS is a type of atomic emission analysis using high-power laser pulses to collect and analyze samples [97, 98]. Laser sampling occurs as nanosecond pulsed laser radiation interacts with the sample surface to induce laser plasma with atomization of the material and excitation of electron transition spectra of atoms and ions. To carry out qualitative and quantitative analyses, characteristic spectral lines in the resulting emission spectrum of the laser plasma are examined. A distinctive advantage of the method is the possibility of obtaining information about the chemical composition of the sample in any aggregation state and under any conditions if it is possible to deliver laser photons and collect plasma emission photons. Due to such advantages as the possibility of nondestructive testing and multi-element and rapid local analysis, LIBS provides a promising method for implementing chemical composition control [99].

LIBS studies of soil and water. The entry of heavy metals through the soil–crop system is considered to be a predominant route of human exposure to heavy metals from the environment in agricultural areas [100]. The first studies reporting determination of impurities in soil using laser-induced plasma spectrometry were published back in the mid-1990s [101, 102]. The authors demonstrated that the detection limit for toxic metals, such as Cd, Pb, and Cr, by the LIBS method was sufficient to evaluate dangerous levels of pollution. However, a quantitative analysis of the elemental composition of soils proved a difficult task for LIBS due to matrix effects that strongly influence the properties of laser plasma [103]. An effective approach to the improvement of the metrological characteristics of soil analysis was found using a two-pulse LIBS mode [104]. Successive exposure to two nanosecond laser pulses with a microsecond delay between them made it possible to enhance the sensitivity of the analysis (by reducing detection limits) for various soil samples. The standard-free approach for LIBS developed by the group of Prof. Palleschi [105] made it possible to obtain information on the levels of major and minor soil components without the use of standard samples. In this context, the availability of compact portable devices for rapid soil analysis directly in the location of interest becomes of great importance [106].

The LIBS technique is used not only to determine toxic impurities but also to monitor the main macrocomponents on which the nutritional properties of the soil depend. The authors of Ref. [107] demonstrated a quantitative analysis of P, Fe, Mg, Ca, and Na in soils and fertilizers. To improve detection limits and the reproducibility of soil analysis data, static analysis approaches (correlation analysis, principal component analysis, and cluster analysis) are used [108]. LIBS makes it possible to measure the granulometric composition of the soil [109] and even its acidity index [110].

Water used to irrigate agricultural land may also contain heavy elements. In analyzing liquids, LIBS is inferior to the methods of analytical chemistry in terms of reliability of the data obtained. However, the advent of compact and inexpensive instruments over the last decade has stimulated the development of simple methods for the elemental analysis of aqueous solutions. Note that the LIBS of aqueous solutions is complicated by such interfering factors as a shorter lifetime of the laser plasma, a weaker spectral signal, and splashing [111]. To minimize the effects of interfering factors and improve the metrological characteristics of water analysis, various approaches are used for preliminary sample preparation, such as freezing [112], preconcentration using absorbent agents [113], or creating aerosols [114].

LIBS for plant research. The possibility of an express multi-element analysis including light elements as well as the possibility of constructing maps of the distribution of macro- and microelements stimulated work on diagnosing the condition and growth of plants. Note that a direct analysis without preliminary sample preparation is a nontrivial task because of the heterogeneous structure of the samples and the diversity of their physical properties (optical, thermodynamic, mechanical) which significantly affect the properties of the laser plasma and the recorded LIBS signals [115]. To improve the reproducibility of LIBS measurements, various procedures for preliminary sample preparation of plant samples are used. For example, a common practice is to grind plant material to reduce the particle size of the sample and homogenize its surface to increase the representativeness of a single measurement. The crushed and mixed plant material is compressed into tablets to form a flat surface and thereby improve measurement reproducibility [116]. An important factor for obtaining reliable analytical results is control of the power density on the sample surface [117]. Using these approaches, the capabilities of LIBS for determining the content of macro and microelements in sugar cane leaves [118] were previously demonstrated; the content of heavy elements in mustard [119] and sunflower leaves [120] was determined.

Such advantages of LIBS as the possibility of carrying out local analysis due to the small focusing spot of the laser beam on the surface of the sample (diameter up to 10 μm) and quasi-nondestructive analysis (the mass of evaporated material per laser pulse does not exceed tens of nanograms) allow the method to be used for mapping the elemental composition in samples [121]. Thus, the authors of Ref. [122] studied the process of absorption and distribution of chromium in various parts of the wheat plant (root, stem, leaves) using LIBS mapping. It was demonstrated that more chromium accumulates in the leaves and roots than in the stem. A large number of studies on the distribution of elements in various plants and their separate parts using different approaches were carried out by Kaiser's group [123, 124]. Approaches to calibrating a LIBS system for the quantitative analysis of heterogeneous plant samples of soybean meal using mapping were presented in Refs [125,126].

LIBS for food analysis. LIBS has already successfully proven itself for the analysis of various food products. For example, Bilge et al. demonstrated the ability of LIBS to determine calcium concentration in flour [127]. Martelli et al used LIBS in combination with chemometric methods to classify wheat grain tissues [128]. Control of the content of the main elements and impurities was carried out using powdered milk samples and infant formulas [129]. The possibility of classifying red wines with a protected designation of origin using a combination of LIBS measurements and neural networks was demonstrated [130]. The authors of [131] gave evidence of good prospects for using LIBS for sorting poultry meat by calcium content on a production line. A large number of papers are devoted to the use of LIBS to assess the content of macro- and microelements in various types of rice [132, 133]. Continuous monitoring of food production at a farm or on the production line requires several hundred measurements per day, so it is necessary to have compact instruments for rapid analyses. The flourishing production of compact LIBS devices [134], including domestically developed ones, makes them promising for use on modern farms focused on highly efficient production of high-quality food products.

6. Application of Mueller polarimetry in biological and agricultural diagnostics

Optical methods based on recording transmitted or scattered light are used for the purpose of nondestructive diagnostics [135–138]. However, optical instruments often measure only the intensity of light without taking into account changes in its polarization state. Methods that detect changes in polarization can provide additional information about the environment under study and improve the accuracy of measurements. The Mueller matrix (MM, 4×4) most fully describes the interaction of an arbitrary object with fully or partially polarized electromagnetic radiation. Therefore, the existing polarimetric methods can be generalized by the Mueller matrix formalism; this generalization is called Mueller polarimetry (MP) [139–141].

In the case of dispersed media, the light scattering matrix (LSM) defined as the Mueller matrix contains the most complete information about light-scattering particles available for static scattering. MRS elements as functions of the scattering angle also depend on the wavelength of probing radiation, optical properties, and size distribution of the dispersed substance [142–144]. In the special case of spherical particles, it has a block-diagonal shape:

$$\mathbf{M} = \begin{vmatrix} M_{11} & M_{12} & 0 & 0 \\ M_{21} & M_{22} & 0 & 0 \\ 0 & 0 & M_{33} & M_{34} \\ 0 & 0 & M_{43} & M_{44} \end{vmatrix},$$

where $M_{11} = M_{22}$, $M_{12} = M_{21}$, $M_{34} = -M_{43}$, and $M_{33} = M_{44}$. The physical meaning of the element $M_{11}(\theta)$ is the scattering indicatrix, i.e., the angular distribution of scattered light intensity (θ is the scattering angle).

Diagnostics of particles using MM is carried out, in essence, by mathematical processing of its elements measured for the scattering, transmission, or reflection of light in accordance with the selected structural model of the medium or sample under study in order to extract the values of its microphysical parameters [141]. The simplest structural model is a collection of spherical particles. However, the particles can be either solid elements or clusters and also have different shapes and sizes to which the MM is also sensitive. To solve the inverse problem of the MM, various mathematical approaches are used. Most often, they are decompositions of directly measured MMs [140, 145], particularly using the group theory [146] or stochastic Monte Carlo simulations [147–150]. The Monte Carlo simulations of MMs for multiple scattering media are very important when interpreting MMs measured for turbid media such as biological tissues [151, 152].

Optical methods and nondestructive diagnostic devices can be divided into four groups. The first includes methods based on measuring the angular distribution of light scattered by a sample (scatterometers) and polarization characteristics of the scattered light. The second group is formed by systems for visualizing densely structured objects, such as biological tissues, in particular those that reflect backscattered light from a deep-lying narrow layer using low-coherence interferometry. This is an optical coherence tomography (OCT) technique. The third group includes spectrophotometers that measure the dependence of the transmission/absorption of light by a sample on the light wavelength, i.e., spectral methods. The fourth group contains fluorescence spectrometers. Schematic features of all four groups and conditions for their application are analyzed below taking into account relevant literary sources. The general principle of modifying the optical design by surrounding the test sample with polarimetric blocks to expand the measurement capacity from a single light intensity to the full Mueller matrix is applicable to all methods.

The simplest instruments are Mueller-polarimetric devices. A Mueller polarimeter typically consists of a light source (IS), a polarization state generator (PSG), a test sample cell (O), a polarization state analyzer (PSA), and a photodetector (PD). Light sources can vary depending on the purpose for which a given polarimetric instrument is designed and the accuracy of measurement, from broadband lamps and superluminescent diodes [153] to lasers [154]. A PSG is a transmittance optical system intended to generate any arbitrary polarization state (usually elliptical) and is used to convert polarization of source radiation that is initially unpolarized or has a constant polarization into a set of polarized light states necessary to measure the Mueller matrix of an arbitrary object. PSGs differ in design. The most common PSG in polarimetric instruments consists of a combination of phase modulators, phase plates, and a linear polarizer. A PSA is also a combination of phase optical elements (phase modulators, phase plates) and a linear polarizer which serves to measure the components of the Stokes vector of radiation emerging from an object.

Scatterometry is a nondestructive diagnostic method based on the measurement of light scattering by a sample. This method measures the angular intensity distribution of light scattered by the sample. Its advantages are the relative simplicity and flexibility of choosing light sources and photodetectors. One can use both monochromatic lasers with different wavelengths and broadband lamps. A simplified diagram of a scatterometer using MP is shown in Fig. 3.

Spectrophotometry studies the spectral properties of electromagnetic radiation reflected or transmitted by a material using a special device (photometer) that measures intensity at different wavelengths. The most widely used spectrophotometers operate in the near-infrared (IR), visible, and ultraviolet (UV) ranges, although microwave and X-ray spectrophotometers also exist. Spectrophotometers come as single-beam and double-beam devices. A single-

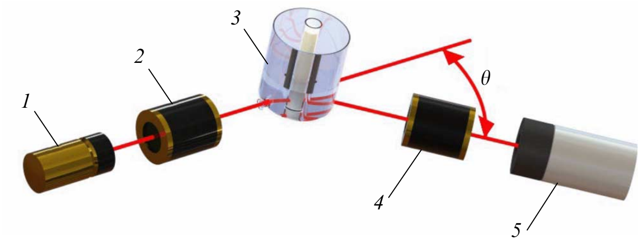

Figure 3. Simplified diagram of a Mueller-scatterometer: *1* — laser, *2* — PSG, *3* — sample, *4* — PSA, *5* — photodetector.

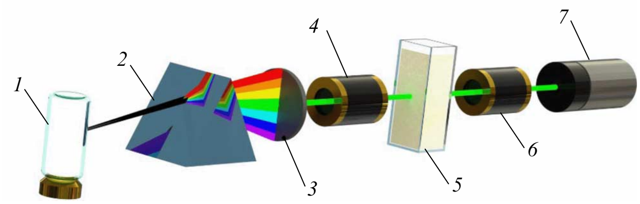

Figure 4. General diagram of a single-beam scanning Mueller spectropolarimeter: *1* — light source, *2* — monochromator, *3* — aperture, *4* — PSG, *5* — sample, *6* — PSA, *7* — photodetector.

beam spectrophotometer measures the relative intensity of a light beam before and after the introduction of the test sample. A dual-beam spectrophotometer compares the intensity between two light paths, one directed at the test sample and the other at a reference. In addition, spectrophotometers can be divided into scanning and matrix types. A scanning spectrophotometer uses a single detector and a moving dispersive element, while an array spectrophotometer uses an array of detectors and a stationary dispersive element. The combination of spectrophotometry with MP makes it possible to measure optical anisotropy spectra, which provides additional information about the configuration of complex organic molecules and, for example, the secondary structure of biopolymers. Such combined systems are called Mueller spectropolarimeters; a possible system including a single-beam scanning spectrophotometer is presented in Fig. 4.

Mueller polarimetric imaging (MPI) is based on measuring the spatially dependent polarization properties of samples in the form of two-dimensional patterns of MM elements, usually using array photodetectors such as CCD cameras [155–157]. Depending on the properties of the sample and the structures of interest inside it, Mueller-matrix images can be recorded in transmission [156] and reflection [157] or backscattering [155] configurations. Thin sections of tissue can be imaged using transmission Mueller microscopy while, for bulk tissue samples, backscatter observation is most appropriate. MPI can provide important details of tissue microstructure [155], cellular functions, and interactions between cellular structures [157].

Optical coherence tomography (OCT) refers to a class of optical imaging techniques used to obtain micrometer resolution of 2D and 3D images of optically scattering media such as biological tissues. This method is based on short coherence length interferometry typically implemented in the near-infrared range (NIR, 800–1300 nm). Unlike classical laser interferometry with a long coherence length, interference in OCT occurs within a few micrometers due to the use of light sources with a wide bandwidth. Time-domain

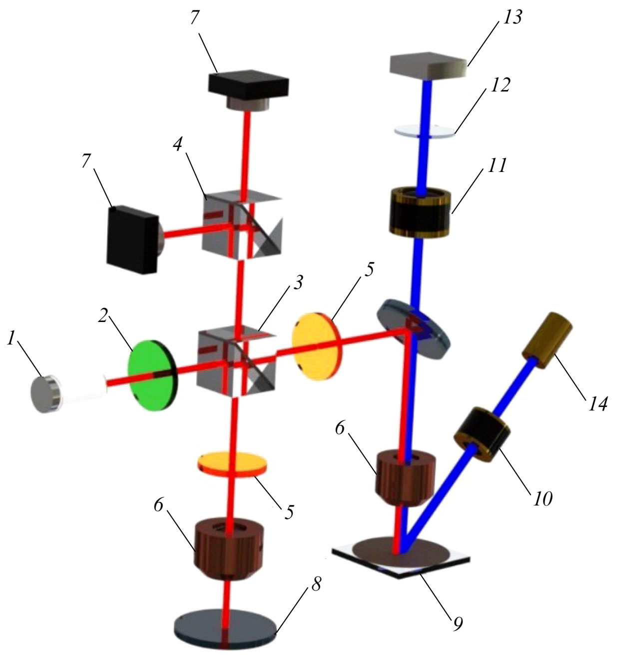

Figure 5. Combined scheme of PS-OCT and MPI: *1* — low-coherence light source, *2* — linear polarizer, *3* — nonpolarizing beam splitter, *4* — polarizing beam splitter, *5* — four-wave plates, *6* — lenses, *7* — photodetectors, *8* — mirror, *9* — sample, *10* — PSG, *11* — PSA, *12* — lens, *13* — CCD camera, *14* — laser.

optical coherence tomography is based on the interference of low-coherence probing optical radiation backscattered from inhomogeneities in the medium and reflected from a reference mirror. In OCT, the coherence condition for reference and backscattered light can be satisfied within a thin layer of the sample. By adjusting the path delay of the reference beam, it is possible to scan the entire depth of the sample and thus obtain a volumetric image.

The use of polarimetry with OCT does not necessarily imply the measurement of the Mueller matrix. Thus, in [158], two approaches were compared: polarization-sensitive OCT (PS-OCT) and Mueller-OCT (M-OCT). These approaches solve slightly different problems: for example, PS-OCT allows obtaining detailed images of the sample under study, while M-OCT makes it possible to investigate its properties. Complete information about the optical properties of tissue can be obtained by integrating MPI and PS-OCT. Figure 5 shows the combination of PS-OCT and MPI proposed in [158].

Fluorimetry is a highly sensitive method based on measuring fluorescence intensity, i.e., the ability of a substance to emit light when absorbing external electromagnetic radiation predominantly at a wavelength greater than that of the absorbed radiation. The principles underlying the use of fluorescence polarization to study protein-protein and protein-DNA interactions are outlined in [159]. The polarization properties of fluorescence contain potentially valuable information about the chemical composition, molecular structure, and orientation, as well as the local environment, of the fluorescent elements. A method that combines fluorimetry and polarimetry can be called fluoripolarimetry. The method turned out to be a powerful diagnostic tool while being quite simple and inexpensive. A typical setup of a polarimetric fluorescence spectrometer with MM measurement is shown in Fig. 6.

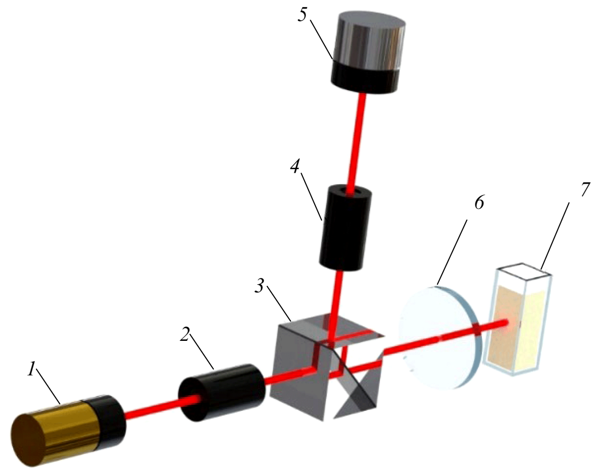

Figure 6. Typical diagram of a Mueller fluorescence spectrometer: *1* — laser, *2* — PSG, *3* — beam splitter, *4* — PSA, *5* — spectrometer, *6* — lens, *7* — sample.

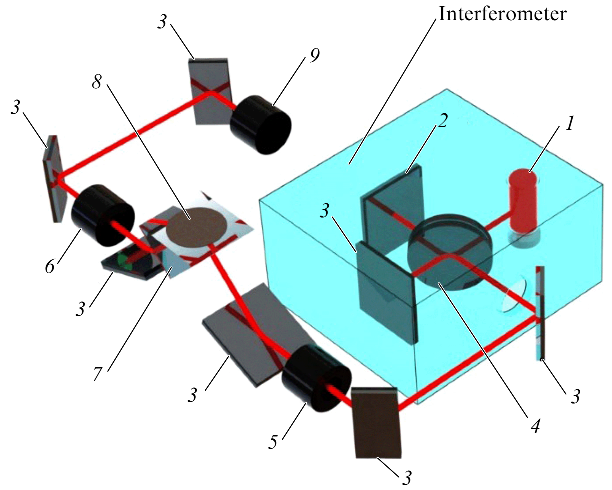

Figure 7. Mueller-ATR-FTIR spectrometer for measuring IR spectra of Mueller matrix elements of a sample placed on an ATR surface: *1* — IR emitter, *2* — movable mirror, *3* — mirrors, *4* — beam splitter, *5* — PSG, *6* — PSA, *7* — ATR optical element, *8* — sample, *9* — photodetector.

Ellipsometry is a highly sensitive method for determining the optical parameters of reflective samples based on the relative change as a result of reflection of the amplitudes and phases of the electric field components of an electromagnetic wave parallel and transverse to the plane of incidence.

Spectroellipsometry in the IR range finds application for the analysis of multicomponent organic materials with characteristic IR absorption lines. To work with thick samples, a standard Fourier transform infrared (FTIR) spectrometer can be equipped with an attenuated total internal reflection (ATR) device combined with achromatic polarimetric elements for measuring the reflection of MM of bulk materials in the spectral range from 3 to 14 μm [160]. A diagram of a Mueller-ATR-FTIR spectrometer for measuring the IR spectra of elements of an MM sample placed on the surface of an ATR element is shown in Fig. 7.

The existing MM implementations are suitable for characterizing organic and microbiological dispersions, surface structures, and biological tissues by obtaining polarization-contrast images and microphysical properties (particle size distribution, fractal and anisotropic properties) of the

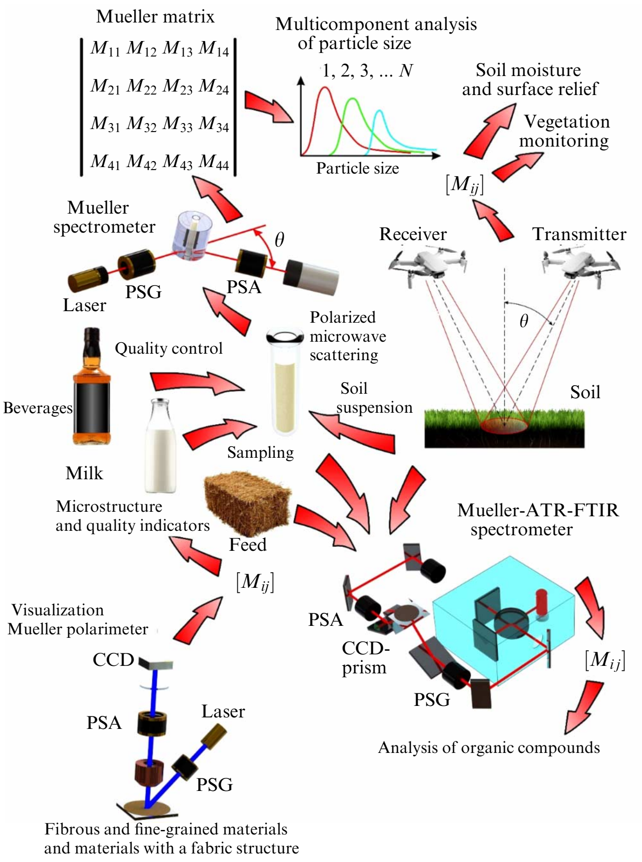

Figure 8. Main applications of MP in agriculture.

measured MMs. In addition, MP can be used to analyze the content of organic components in agricultural materials and products (milk and beverages, feed, etc.), as well as to diagnose soil and vegetation properties. From the MM, material-specific parameters can be derived that can serve as indicators of the quality of agricultural products. Thus, MP can be considered an effective diagnostic tool for biological and agricultural research.

The above examples of MP implementation show that MP is a powerful tool for noninvasive diagnostics of bio-organic systems, especially in combination with other optical methods, significantly expanding their potential. The above review of MM installations makes it possible to systematize optical methods supplemented by MM measurements into groups depending on

- sample geometry: volumetric (Mueller-scatterometry, Mueller-spectrophotometry, Mueller-fluorometry) or surface (Mueller-OCT and Mueller-ellipsometry);
- properties of incoming radiation: spectral (spectrophotometry and spectroscopic Mueller-scatterometry, Mueller-fluorometry and Mueller-ellipsometry) or nonspectral (Mueller-OCT and single-wavelength Mueller-scatterometry, Mueller-fluorimetry, and Mueller-ellipsometry);
- information received: visual (Mueller-OCT and other polarization-sensitive imaging methods) or structural (all methods that measure MM followed by restoration of the microphysical parameters of the sample using inverse analysis);
- operating conditions: stationary or mobile.

The main agricultural applications of MP are systematized in the form of the block diagram shown in Fig. 8.

7. Application of optical methods for the analysis of the quality of milk and feed

Quality control of milk and dairy produce is an important issue in the modern dairy industry. An important task is to find out technological solutions for the express (without delay) analysis of raw milk during the milking procedure. A detailed review of optical methods used to determine milk composition is presented in [161]. The most popular method for the assessment of milk quality appears to be IR spectroscopy in the mid-infrared range ($\sim$ 50% of studies). The most frequently analyzed components characterizing the quality of milk are the concentration of fat [162] and total protein, carbohydrates (lactose) [163], and casein [164]. A small number of studies have examined the possibility of identifying somatic cells (an indicator of mastitis) [165, 166]. The possibility of detecting melamine [167] and lead [168] in milk using mid- and near-infrared spectroscopy has also been reported.

A serious problem associated with the analysis of raw milk is the aggregation of fat micelles and protein globules, which hinders accurate diagnosis due to scattering [169]. The presence of water in milk complicates NIR spectroscopic analysis; in turn, the presence of micro- and macro-bubbles of air also creates interference [170]. Milk contains about 88% water, which produces very strong bands in the near-infrared region around 960, 1440, 1950, and 2076 nm, overlapping with some bands of interest [171]. The IR spectroscopic method requires precise calibration and selection of the optimal algorithm for interpreting the obtained spectra. The most commonly used models are those constructed using partial least squares (PLS) regression [172]. To improve the quality of measurements, it is necessary to use more complex models with the preliminary processing of spectral data [173]. It should be noted that the vast majority of known IR installations operate only with pre-selected samples; in-line measurements are practically impossible [161].

The Institute of General Physics of the Russian Academy of Sciences has developed a sensor for determining the fat content in a milk flow (Fig. 9a) which has a cylindrical geometry of the measuring chamber compatible with milk pipelines (Fig. 9b). The sensor is based on measuring the angular distribution of light scattered by milk flowing inside an optically transparent cylindrical glass tube using a visible wavelength laser diode coupled to an axial photodiode array [174]. Currently, the sensor is integrated into the first Russian robotic milking machine, developed by the VIM Federal National Research Center. Along with measuring the content of the main milk components, the detection of large-scale impurities such as somatic cells is also an urgent task. Experiments show that, starting from a certain concentration level (10^5 ml^{-1}), the presence of large impurities in milk leads to a relative change in the forward scattering intensity compared to pure milk.

Obviously, the efficiency of dairy production can be significantly increased through the introduction of inexpensive and compact devices [175]. In accordance with the requirement to use control devices that do not lead to a significant drop in pressure in the milk hose, when developing milk quality sensors for dairy farm equipment, optical diagnostic methods are especially promising, since they allow contactless and nondestructive diagnostics with high sensitivity and speed [138, 176, 177].

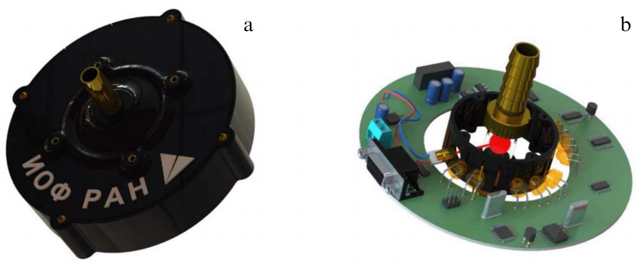

Figure 9. Laser scatterometric sensor developed at the Institute of General Physics of the Russian Academy of Sciences (conceptual model): (a) general view of the sensor; (b) sensor layout.

As is known, the quality and volume of dairy products depend on the composition and balance of feed consumed by animals. In this regard, special attention is paid to the control of feed for farm animals [178]. According to the literature, the method of reflectance spectroscopy in the near-IR range is predominantly used for feed analysis ($\sim$ 90% of studies), and only a few studies have used spectroscopy in the mid-IR region. At the same time, the most frequently analyzed components of farm animals' feed using NIR spectroscopy that determine their energy value and digestibility are the levels of crude protein (CP), fats, neutral detergent fiber (NDF), acid detergent fiber (ADF), water-soluble carbohydrates (WSCs), and total nitrogen (N). It is noteworthy that other optical methods, including luminescence analysis, are also used to analyze the composition of feeds. In particular, the work of Pavkin's laboratory suggests the possibility of monitoring the homogeneity of feed mixtures when recording photoluminescence in a wavelength range of 390–540 nm (excitation wavelengths of 362 and 424 nm) [179, 180]. Details of the use of optical methods for feed control can be found in Ref. [161].

8. Production and application of nano-sized objects in agriculture and the food industry

The antibacterial properties of metals have been known since ancient times. A wide range of metals exhibit antimicrobial activity: Ag, Al, As, Cd, Co, Cr, Cu, Fe, Ga, Hg, Mo, Mn, Ni, Pb, Sb, Te, Zn [181]. Currently, the interest in nanoparticles (NPs) of metals and their oxides as compounds with antibacterial potential is growing significantly [182]. The antimicrobial properties of NPs are primarily determined by the antimicrobial properties of the elements in their composition. For example, in NPs of silver and its oxides, silver ions Ag^+ act as antibacterial agents [183]. At least five mechanisms of antibacterial activity have been described for metal oxide NPs (Fig. 10).

The first mechanism is the direct binding of nanoparticles to the bacterial cell wall with the disruption of its integrity and direct damage to the cell membrane and cytoplasmic components [184]. It is assumed that, after penetration of metal oxide NPs into a bacterial cell, metal ions are released that exhibit bactericidal activity mediated through the mechanisms described below.

The second mechanism of toxicity is the binding of metal ions (Ag^+, Zn^{2+}) to the SH groups of proteins with subsequent disruption of their functions. In particular, silver and iron-induced inactivation of bacterial enzymes, especially respiratory chain dehydrogenases, has been described [185]. This, in turn, inhibits the synthesis of adenosine triphosphoric acid (ATP) and effects the energy balance of cells [186]. In addition, metal oxide NPs are in some cases capable of releasing O_2, which can also exhibit antibacterial activity [187].

The third mechanism is the development of oxidative stress. Two pathways for the development of oxidative stress have been described. One is the generation of reactive oxygen species (ROS) in the Fenton reaction or a similar one [188]. The other is a decrease in the enzymatic activity of the antioxidant system (SOD, catalase, glutathione reductase) due to the binding of metal ions to the mercapto (–SH), amino (–NH), and carboxyl (–COOH) groups of proteins [189]. ROSs, in turn, cause modification of proteins and have a genotoxic effect [190]. In addition, metal ions can accelerate lipid peroxidation and disrupt lipid-protein interactions in the bacterial membrane [191]. The increased ROS production leads to the destruction of the cell wall and biofilms of both Gram-positive and Gram-negative bacteria [192].

The fourth mechanism of antibacterial activity of metal oxide NPs is genotoxicity caused by the interaction of metal cations not only with proteins but also with phosphoric acid residues in DNA molecules [193]. In particular, silver compounds from Ag_2O NPs or Ag NPs can bind to the N7 atom of guanine in DNA and thereby affect replication and cell division [194]. Metal oxide NPs can interfere with normal gene expression in bacteria. Notably, they reduce the expression of genes responsible for antibiotic resistance in antibiotic-resistant bacteria cultured from operating rooms [195].

The fifth mechanism is photocatalytic activity, which is expressed as increased generation of ROS in the presence of light [196]. It is noteworthy that composites of NPs made of several oxides, e.g., Ag_2O/TiO_2 or Ag_2O/ZnO, demonstrate an increased photocatalytic activity compared to NPs consisting of only one oxide [197].

Methods for the synthesis of metal nanoparticles and their oxides are numerous and include chemical, physicochemical, and physical ones. Methods of chemical synthesis include precipitation, thermal decomposition, chemical vapor deposition, low-temperature synthesis, sol-gel method, microemulsion, and synthesis using a polymer as a matrix [198, 199]. The physicochemical methods include electrochemical, hydrothermal, and sonochemical techniques [200, 201]. Physical methods of synthesis are laser ablation in a solvent or gas, microwaves, the ultrasonic method, electrocorrosive dispersion, and electrical explosion of two twisted wires [202–208]. The antimicrobial effect depends on the conditions of NP synthesis and their size and shape. As a rule, the antimicrobial activity of NPs increases with a decrease in their size [209]. Round or star-shaped NPs are often the most effective against bacteria [182].

Metal/metal oxides nanoparticles can be used in various fields, including the food industry [210]. Applications in the food industry can include the development of new biodegradable packaging with antibacterial properties or protective coatings for work surfaces, particularly in meat processing [211, 212]. The addition of metal oxide NPs to a polymer matrix makes it possible to create a new generation of materials with antimicrobial properties. Specifically, metal oxide NPs can be added to a polymer matrix of borosiloxane, PLGA (poly-lactic-co-glycolic acid), or fluoroplastic (polytetrafluoroethylene) [212–214]. Nanomaterials based on borosiloxane can be used in the manufacture of sportswear,

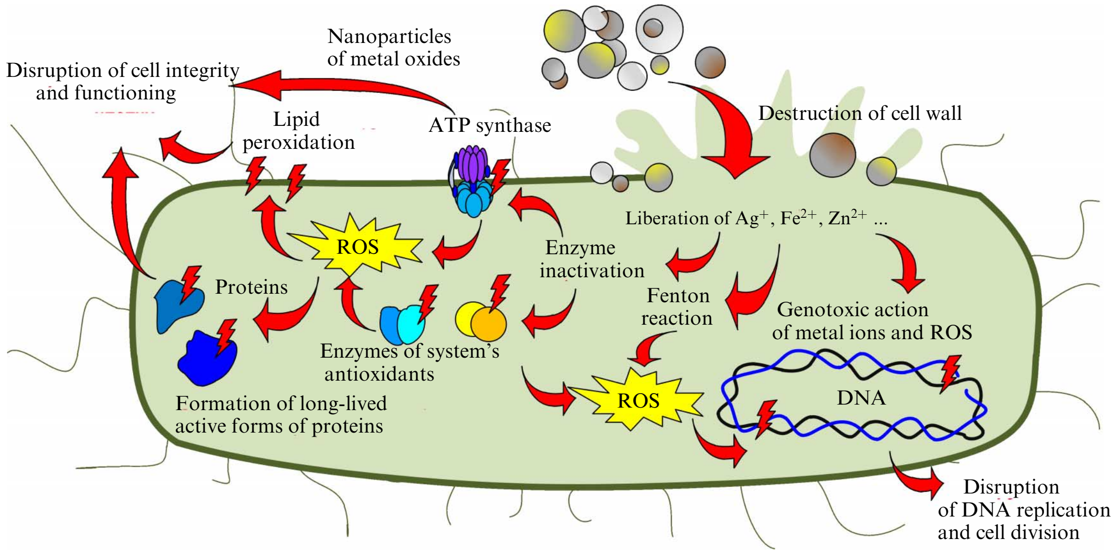

Figure 10. Main mechanisms of the antibacterial action of metal oxide NPs.

protective self-healing coatings for device, and other applications: screens, prosthetics, biomedical devices, and reusable dry disinfectants [215]. The addition of metal oxide NPs to the PLGA polymer matrix will make it possible to create materials for biomedical applications, including prosthetics [216]. It is noteworthy that the nanocomposite of silver oxide NPs with PLGA exhibits pronounced bacteriostatic properties at NP concentrations less than 0.1% by weight, i.e., lower than that of other nanomaterials with silver oxide NPs, in particular, NP/chitosan-type nanomaterials [217, 218]. A nanocomposite of ZnO, Ag_2O, or iron oxide NPs with fluoroplastic is synthesized in the form of a liquid phase, convenient for application to various surfaces, including sputtering. After hardening of the composition, a strong protective film is formed which significantly inhibits the growth of epidemiologically significant Gram-positive (*L. monocytogenes, S. aureus*) and Gram-negative (*P. aeruginosa, S. typhimurium*) bacteria [211, 219]. Moreover, the resulting composite does not have a cytotoxic effect on eukaryotic cell cultures [211, 220]. A similar nanomaterial has found application in the food industry, e.g., for the treatment of cutting boards in meat processing plants [219, 220].

9. Plasma technologies in agriculture

Since the beginning of the 20th century, the physics of discharges as a source of low-temperature plasma (LTP) under atmospheric pressure has been in the focus of plasma technology research, the development of energy supply systems, and the use of LTP in the processes of purification of drinking water and air. Significant progress in the development of technologies for creating effective LTP generation systems was achieved beginning in the early 1990s. As a result, new areas of application have emerged, including agriculture, food safety, and security [221]. The effect of LTP on biological objects is complex and multifactorial. The main contribution comes from the use of the flows of charged and chemically active particles, infrared radiation (heat), electric fields, mechanical waves, and ultraviolet radiation. Several key effects of such synergistic action can be identified for agriculture (more precisely for plants in general and planting material). To begin with, the pre-sowing treatment of seeds with LTP can stimulate their germination, increase the yield of seedlings, and improve their further growth and development [222]. The exposure to LTP results in the activation of physiological processes and improves permeability of cell membranes, which, in turn, contributes to more efficient absorption of moisture and nutrients. Second, plasma treatment can be used to prevent and control plant diseases, kill bacteria and fungi, and disinfect seeds and soil [223]. Third, treatment of adult plants with LTP can increase their chlorophyll content, accelerate photosynthesis, enhance fruiting, promote root growth, and improve plant resistance to a variety of stressful factors [224].

The existing sources of low-temperature plasma for use in agriculture are usually prototypes of devices with limited possibilities for application in field conditions, which place increased demands not only on the level of personnel qualifications but also on electrical safety, conditions of the premises, etc. The disadvantages of such devices include the uneven impact of plasma on objects of complex shape, which reduces the general effectiveness and the yield of high-quality (suitable) products. Another unresolved problem is the comparison of the effects of low-temperature plasma generators of various types and characteristics as well as the extrapolation of these results to all popular types of agricultural plants. Taken together, these factors, combined with technical difficulties in scaling the technology, slow down the introduction of plasma treatment of plants and planting material into the real sector of the economy [225].

An alternative, easily scalable way to use LTP sources in agriculture is to produce plasma-activated water (PAW) or saline (PAS) solutions for the subsequent treatment of biological objects. It requires the study and analysis of reactions between air and water environments under the influence of LTP gas discharges. Currently, a large number of methods are available to study liquids and radical reactions in them [226–232]. It is known that the plasma action on a liquid gives rise to a variety of secondary active particles, including those with low reaction rate constants. During the interaction of long-lived ROS and reactive nitrogen species (RNS) contained in PAW and PAS [233–235] with biological objects, a cascade of physicochemical processes having a concentration-dependent nature is observed. PAW and PAS remain chemically active for a relatively long time and can be an environmentally friendly alternative to chemical fertilizers. The study of the production of RNS and ROS in liquids is necessary to characterize and standardize any laboratory or industrial source of LTP.

The operation of the main types of LTP sources widely used during recent years in agrobiology is based on (1) corona discharge, (2) spark discharge, (3) underwater electric discharge, (4) discharge with a dielectric barrier, and (5) generation of a plasma jet.

A corona discharge occurs as a result of ionization of the air accompanied by glow under the influence of a highly inhomogeneous electric field near the conductor. It takes place only close to one of the electrodes, and the glow of the corona does not spread over the opposite electrode, which can be located at a considerable distance; its role can be played by the object being treated. Corona discharges are widely used to purify gases from dust and contaminants, as well as in ozonizers. When exposed to a corona discharge, the water surface changes its chemical composition [236, 237]. The disinfecting effect of the corona discharge plasma on fungal diseases of winter wheat and winter barley seeds was demonstrated in [238]. A study of the action of corona discharge on dispersed media (fertile soil, clay, sand) [239] demonstrated not only a significant change in electrical conductivity, particle size, and macroelement composition but also an increase in the content of nitrogen-containing components, leading to an improvement in soil fertility.

A spark discharge occurs between electrodes located at some distance from each other. The object being processed can act as one of them. The power of the power source must be insufficient to maintain an arc or glow discharge. In a system with direct action of the spark discharge where a piezoelectric transformer is used as an electrode (the CAPKO multifunctional source was developed at the Prokhorov General Physics Institute, Russian Academy of Sciences (GPI RAS)), one of the operating modes makes it possible to initiate a spark discharge above the surface of the liquids [240, 241]. The one-time volume of a liquid exposed to the plasma action does not exceed 100 ml, and the power consumption of the source is below 10 W. This energy-efficient technique makes it possible to activate liquids of various compositions and thereby generate ROS and RNS. To produce a large volume of PAS for agricultural applications, the GPI RAS has developed a modular multi-spark ring reactor that allows both processing of a given volume of the liquid and continuous processing in a flow mode [242]. The installation implements a high-voltage pulse-periodic multielectrode discharge in the liquid with gas injection into the interelectrode gaps. Due to the high energy and sufficiently long pulse length during each interval (1.6 J; 1.5 μs), it is possible to achieve a relatively high PAS generation rate. Depending on the operating modes, the injected gas, the electrode material, and the initial liquid composition, it is possible to produce PAS with a wide range of ROS, RNS, dissolved metal, and nanoparticle concentrations.

An underwater electrical discharge is usually formed in a pulsed mode by an electrode immersed in a liquid. Due to electrochemical processes and overheating of the liquid, the discharge occurs in vapor-gas bubbles near the surface of the electrode as well as in the air bubbles supplied through tubes to the discharge area if necessary. The process is accompanied by the emission of electrons from a cathode under the influence of ion impacts and photoelectron emission. Due to erosion of the electrode material, PAS contains nanoparticles, dissolved metal ions, and their compounds. One of the options for implementing this PAW generation scheme is presented in Ref. [243], where high concentrations of RNS and ROS in aqueous solutions were obtained using carbon electrodes and additional air injection. This resulted in a better germination of cucumber (*Cucumis sativus*) seeds treated with PAW than from the control.

A more productive reactor was developed at the GPI RAS under the leadership of Danileiko. The design of the reactor is based on similar principles: two electrodes (active and passive) are immersed in a vessel containing an electrolyte [244]. The electrodes can be made from various materials (e.g., the active electrode from platinum, the passive one from pyrolytic graphite). They are connected to a high-frequency generator capable of operating in a wide frequency range, and the power put into the discharge is sufficient to form a vapor-gas bubble at the active electrode and ignite the discharge in the vapor phase [245]. An electrolyte is used as the liquid to be treated; it is a 1–5% aqueous salt solution (NaCl, KNO_3, etc., depending on the purpose). A freshly prepared NaCl-based solution has good disinfectant properties, as was demonstrated in the creation of a low-temperature knife sterilizer for meat production [246]. Other devices with the use of an underwater electric discharge proposed by the authors are capable of maintaining conditions under which chemically active compounds are retained fairly long in solutions. At the same time, a slow destruction of the active electrode is observed with the formation of nanoparticles having a characteristic size of 10–20 nm. Solutions obtained in such devices are often used diluted (from 1:100 to 1:2000) for watering or filling hydroponic, aeroponic, and fog generating systems. The effectiveness of PAS has also been demonstrated using the example of sorghum seed germination [247]: the plant demonstrates resistance to drought, and extensive field experiments have been carried out in the saline semi-desert of the Northern Caspian Sea area. Also, PAS can promote better fusion of plant sections during grafting [248] and also have a significant effect on the Ca content in apples during watering [249], which may have a positive effect on the duration of fruit storage.

Dielectric barrier discharge (DBD) is a simple and relatively safe procedure for plasma generation, since in this type of discharge conduction current and charge transfer are blocked by the dielectric barrier. It is a series of fast-flowing microdischarges in a gas provided that at least one of the electrodes is separated from the gas by a dielectric barrier. The dimensions of the electrodes in the DBD significantly exceed the width of the discharge gap, which varies from fractions of a millimeter to several centimeters. Such discharges are widely used for the treatment of large surfaces and in agrobiology for direct treatment of planting material or plant surfaces for the purpose of disinfection and control of pathogens.

Studies [248, 250] describe an original technique for grafting garden plants (pears and cherries) using DBD. It was shown that plasma treatment of scion and rootstock sections subsequently leads to a better formation of the grafting zone, a more rapid increase in plant biomass, and, as a consequence, a reduction in the time it takes to bring the plant to market. Using impedance spectroscopy [251, 252], it was shown that, after plasma treatment, the formation of a more developed vascular system in the grafting zone is observed.

An atmospheric pressure plasma jet is created by plasma generators based on electric arc discharges and high frequency induction discharges. The electric arc discharges have powers ranging from hundreds of W to several MW, and the generated plasma contains electrode particles resulting from erosion. Subsequently, generators were developed using high and ultrahigh frequency induction discharges. Such generators make it possible to isolate the discharge from the electrodes and walls of the discharge chamber and produce plasma without contact with the elements of the plasmatron. These systems are usually used to solve environmental problems that require high temperatures and significant energy consumption. More economical plasma jets are created using a spark discharge or a dielectric barrier discharge with a flow of inert gases (for example, argon and helium). They are most widespread in the field of medicine.

A series of papers [253, 254] describes a multielectrode coaxial plasmatron as a source of low-temperature plasma with a large processing area. The discharge is initiated in a flow of an inert gas using microwave radiation with a frequency of 2.45 GHz and a power in the torch of $\sim$ 100 W. Another team created a water activation installation based on a microwave plasmatron for a wide range of biological applications [255]. The energy source for plasma generation is a 1.2-kW magnetron operating at a frequency of 2.45 GHz in a continuous generation mode. The PAS obtained in this installation diluted in distilled water to a concentration of 0.5–1.0% increases the germination energy, and protects cotton, wheat, and strawberry seeds from fusarium and hyperthermia [256].

Overall, research on the use of low-temperature plasma and plasma-activated solutions (PASs) in agriculture demonstrated the high potential for increasing crop yield and quality, reducing plant diseases, controlling pests and pathogens, and improving tolerance to stress conditions. Plasma technologies represent an environmental trade-off that can reduce the use of chemical fertilizers and pesticides. Further research and practical implementation of plasma technologies can have a significant impact on agricultural production.

10. Optical methods for detecting phytopathogens

Plant diseases are considered a risk factor because they are difficult to detect and identify in the early stages [257]. Phytopathogens can impact both plants and harvested crops. Timely diagnosis can save more than 50% of the total crop yield worldwide as well as save on the use of pesticides through the early isolation of diseased plants and, as a result, preventing the spread of infection. This section provides an overview of recent advances in optical techniques used in plant pathology. Optical methods are characterized by speed, ease of use, the ability to screen large areas, low price, and a small number of maintenance personnel. The development of technical means for obtaining optical information, monitoring systems, and computer data processing also contributes to the active introduction of optical methods for the detection of phytopathogens [258].

Spectral imaging, perhaps the most extensive class of methods, is based on the detection of reflected (less often absorbed or transmitted) light interacting with an object. The methods involve capturing images of objects in which each pixel carries spectral information — by increasing the number of spectral bands and reducing their width. There are RGB, multispectral, and hyperspectral imaging (HSI) [259]. It is believed that HSI provides a wealth of information and can detect a wider range of diseases than RGB imaging. However, HSI has disadvantages, such as high cost, complexity of sensors and optical components, a long data acquisition time, and complexity of processing and analysis. An optical system with a spectral visualization-based orientation module was developed for detecting surface damage and contamination of potato tubers [260].

IR spectroscopy. IR spectra are usually roughly divided into three regions: near-IR (NIR) (780–2500 nm), mid-IR (MIR) (2500–25000 nm), and far-IR (FIR) (25,000–300,000 nm). NIR and MIR spectroscopy allows for extracting information about chemical components and creating so-called 'fingerprints.' MIR spectra can be more appropriately used to study fundamental vibrations and associated rotational vibration structures, while NIR spectra can more easily activate overtones or harmonic vibrations. A method for diagnosing fungal infection of the genus Fusarium on the oat variety 'Zalp' was developed using IR spectroscopy [261].

Raman spectroscopy. The main advantage of Raman spectroscopy is the absence of the influence of water on the spectrum, while the disadvantages include possible fluorescence of the sample that can hide the spectrum, as well as intense laser radiation from a source, which can damage the sample. The use of NIR lasers avoids fluorescence of the sample. Typically, IR lasers are used, less frequently green lasers. Shift detection is usually performed in the range of 700–1800 cm^{-1}. The intensity and the shift of lines and sometimes the width of peaks are analyzed. Raman spectroscopy is used to determine mycotoxins from Fusarium fungi on winter wheat seeds [262].

Fluorescent methods. Fluorescence is the phenomenon of re-emission of absorbed light with some loss of energy due to the structural features of the substance. Unlike reflectance spectra, fluorescence spectra are related to the electronic states of molecules. The concentration and chemical modifications of molecules provide insight into the functional state of the plant, so fluorescence measurements are often associated with biochemical and physiological changes induced by pathogens and/or other factors. Fusarium is detected using fluorescent methods [263–265]. Fluorescence spectroscopy is used to detect rot in vegetable and fruit crops [266, 267].

Terahertz time domain spectroscopy is a spectroscopic technique in which the properties of matter are studied using short pulses of terahertz radiation. The THz-TDS method can clearly determine the presence or absence of a pathogen in a plant. It requires quite a long preparation of samples before measurement. It has been shown that the THz-TDS method allows assessing the degree of infection of cereal seeds (oats, wheat, and barley) with fusarium and potato tubers with late blight. Changes are observed in refractive indices, absorption coefficients, and dielectric functions in healthy and infected plants [268]. The THz-TDS method is also applicable for identifying fungal infections of chestnuts [269]. A large number of studies for the detection of plant pathogens using the Hz-TDS method can be expected in the near future [270].

Currently, optical methods are used as empirical, experimental, and exploratory procedures. Many mechanisms underlying optical manifestations of plant diseases remain unclear, and studies aimed at explaining and predicting optical changes of diagnostic significance are insuggicient. Optical methods have undoubted prospects for mass diagnostics of pathogens and plant diseases in the future, but they require further improvement of their instrumental and analytical components.

References

1. Jang S J, Mennucci B *Rev. Mod. Phys.* **90** 035003 (2018)
2. Mirkovic T et al. *Chem. Rev.* **117** 249 (2017)
3. Goldberg D E *Genetic Algorithms in Search, Optimization, and Machine Learning* (Reading, MA: Addison-Wesley Publ. Co., 1989)
4. Holland J H *Adaptation in Natural and Artificial Systems: An Introductory Analysis with Applications to Biology, Control, and Artificial Intelligence* (Ann Arbor, MI: Univ. of Michigan Press, 1975)
5. Vaitekonis S, Trinkunas G, Valkunas L *Photosynth. Res.* **86** 185 (2005)
6. Brüggemann B et al. *J. Phys. Chem. B* **108** 13536 (2004)
7. Trinkunas G, Holzwarth A R *Biophys. J.* **71** 351 (1996)
8. Raszewski G, Saenger W, Renger T *Biophys. J.* **88** 986 (2005)
9. Trinkunas G et al. *J. Phys. Chem. B* **101** 7313 (1997)
10. Adolphs J, Renger T *Biophys. J.* **91** 2778 (2006)
11. Darwish A, Hassanien A E, Das S *Artif. Intell. Rev.* **53** 1767 (2020)
12. Del Ser J et al. *Swarm Evolut. Comput.* **48** 220 (2019)
13. Slowik A, Kwasnicka H *Neural Comput. Appl.* **32** 12363 (2020)
14. Bilal et al. *Eng. Appl. Artif. Intell.* **90** 103479 (2020)
15. Storn R, Price K *J. Global Optimizat.* **11** 341 (1997)
16. Pishchalnikov R Y et al. *Photosynth. Res.* **156** 3 (2023)
17. Chesalin D D, Pishchalnikov R Y *Mathematics* **10** 959 (2022)
18. Pishchalnikov R Y et al. *Phys. Chem. Chem. Phys.* **21** 25707 (2019)
19. Pishchalnikov R *J. Comput. Phys.* **372** 603 (2018)
20. Chesalin D D et al. *Algorithms* **16** (1) 3 (2023)
21. Mukamel S *Principles of Nonlinear Optical Spectroscopy* (New York: Oxford Univ. Press, 1995)
22. Tretiak S, Mukamel S *Chem. Rev.* **102** 3171 (2002)
23. Smirnov A A et al. *Agriculture* **12** 1988 (2022)
24. Semenova N A et al. *Energies* **15** 8076 (2022)
25. Semenova N A et al. *Appl. Sci.* **12** 7190 (2022)
26. Tikhonov P et al. *Agriculture* **12** 1215 (2022)
27. Gudkov S V et al. *Phys. Wave Phenom.* **25** 207 (2017)
28. Chen Y et al. *Front. Plant Sci.* **10** 1563 (2019) https://doi.org/10.3389/fpls.2019.01563
29. Smith H L, McAusland L, Murchie E H *J. Exp. Botany* **68** 2099 (2017)
30. Zhen S, Haidekker M, van Iersel M W *Physiol. Plantarum* **167** (1) 21 (2019)
31. Kreslavski V D et al. *Biochim. Biophys. Acta BBA Bioenerg.* **1859** 400 (2018)
32. Petroutsos D et al. *Nature* **537** 563 (2016)
33. McCree K J *Agric. Meteorol.* **9** 191 (1971–1972)
34. Paskhin M O, Yanykin D V, Gudkov S V *Horticulturae* **8** 885 (2022)
35. Magnani G et al. *Acta Hortic.* **801** 163 (2008)
36. Stagnari F et al. *J. Sci. Food Agric.* **94** 713 (2014)
37. Casal J J, Sánchez R A *Seed Sci. Res.* **8** (3) 317 (1998)
38. Penfield S, King J *Proc. R. Soc. Lond. B* **276** 3561 (2009)
39. Kambalapally V R, Rajapakse N C *Hortic. Sci.* **33** 1028 (1998)
40. Rajapakse N C, Kelly J W *J. Am. Soc. Hortic. Sci.* **117** 481 (1992)
41. Hernández R, Kubota C *Acta Hortic.* **956** 187 (2012)
42. Mishra K, Stanghellini C, Hemming S *Adv. Sustain. Syst.* **7** 2200503 (2023)
43. Shubbak M H *Renew. Sustain. Energy Rev.* **115** 109383 (2019)
44. Lu L et al. *Sustain. Energy Technol. Assess.* **52** (Pt. A) 102077 (2022)
45. Gudkov S V et al. *J. Photochem. Photobiol. B* **213** 112056 (2020)
46. Shen L, Yin X *Nano Convergence* **9** 36 (2022)
47. Ivanyuk V V et al. *Front. Phys.* **8** 616040 (2020) https://doi.org/10.3389/fphy.2020.616040
48. Simakin A V et al. *Appl. Sci.* **10** 8025 (2020) https://doi.org/10.3390/app10228025
49. Shoji S et al. *Sci. Rep.* **12** 17155 (2022)
50. Ke-li Z et al. *Wuhan Univ. J. Nat. Sci.* **7** 365 (2002)
51. Sánchez-Lanuza M B et al. *Materials* **14** 2357 (2021)
52. Yoon H I et al. *Hortic. Environ. Biotechnol.* **61** 999 (2020)
53. Parrish C H (II) et al. *Commun. Biol.* **4** 124 (2021)
54. Wu W et al. *J. Rare Earths* **38** 539 (2020)
55. Chiu Y-H et al. *Catalysts* **9** 430 (2019)
56. Palkina K K et al. *Russ. J. Inorg. Chem.* **45** 515 (2000); *Zh. Neorg. Khim.* **45** 586 (2000)
57. Minich A S et al. *Vestn. Tomsk. Gos. Pedagogich. Univ.* (8(110)) 78 (2011)
58. Fitzmorris B C et al. *ACS Appl. Mater. Interfaces* **5** 2893 (2013)
59. Pu Y-C et al. *J. Mater. Chem. A* **6** 17503 (2018)
60. Powles S B *Annu. Rev. Plant Physiol.* **35** 15 (1984)
61. Grinberg M et al. *Plants* **11** 229 (2022)
62. Ovsyankin V V, Feofilov P P *JETP Lett.* **3** 322 (1966); *Pis'ma Zh. Eksp. Teor. Fiz.* **3** 494 (1966)
63. Yanykin D V et al. *Agronomy* **12** 108 (2022)
64. Burmistrov D E et al. *Appl. Sci.* **11** 10726 (2021)
65. Yanykin D V et al. *Appl. Sci.* **12** 7480 (2022)
66. Yalçin R A, Ertürk H *Biosyst. Eng.* **193** 25 (2020)
67. Campbell P, Green M A *J. Appl. Phys.* **62** 243 (1987)
68. Makarov N S et al. *ACS Nano* **13** 9112 (2019)
69. Marcelis L F M et al. *Acta Hortic.* **711** 97 (2006)
70. MacQueen R W et al. *Opt. Express* **18** (S2) A161 (2010)
71. de Boer D K G et al. *Appl. Phys. Lett.* **98** 021111 (2011)
72. Bulatov M I et al. *Phys. Wave Phenom.* **30** 397 (2023)
73. Chang A et al. *Comput. Electron. Agric.* **141** 232 (2017)
74. Khanal S et al. *Remote Sens.* **12** 3783 (2020)
75. Sishodia R P, Ray R L, Singh S K *Remote Sens.* **12** 3136 (2020)
76. Kior A, Sukhov V, Sukhova E *Photonics* **8** 582 (2021)
77. Weiss M, Jacob F, Duveiller G *Remote Sens. Environ.* **236** 111402 (2020)
78. Neumann G A *Phys. Today* **56** (1) 50 (2003); Bunkin A, Voliak K *Laser Remote Sensing of the Ocean: Methods and Applications* (New York: Wiley, 2001)
79. Wang L et al. *Remote Sens. Environ.* **231** 111223 (2019)
80. Günther K P, Dahn H-G, Lüdeker W *Remote Sens. Environ.* **47** 10 (1994)
81. Lavrov A et al. *Opt. Spectrosc.* **112** 271 (2012)
82. Bunkin A et al. *Laser Phys.* **4** 1198 (1994)
83. Bunkin A F, Pershin S M *Bull. Russ. Acad. Sci. Phys. Suppl. Phys. Vibrations* **61** (3) 164 (1997)
84. Myasnikov A V et al. *Phys. Wave Phenom.* **30** 119 (2022)
85. Fan B et al. *Chinese J. Electron.* **29** (2) 199 (2020)
86. Zhao X et al. *IEEE Sensors J.* **20** 4901 (2020) https://doi.org/10.1109/JSEN.2020.2966034
87. Lednev V N et al. *Bull. Lebedev Phys. Inst.* **50** (3) 103 (2023); *Kratk. Soobshch. Fiz. Fiz. Inst. Ross. Akad. Nauk* (3) 40 (2023)
88. Lednev V N et al. *Photonics* **9** 963 (2022)
89. Lu J et al. *Appl. Opt.* **59** (10) C1 (2020) https://doi.org/10.1364/AO.59.0000C1
90. Grishin M Ya et al. *Dokl. Phys.* **66** (6) 153 (2021); *Dokl. Ross. Akad. Nauk Fiz. Tekh. Nauki* **498** 3 (2021)
91. Grishin M Ya et al. *Dokl. Phys.* **66** (10) 273 (2021); *Dokl. Ross. Akad. Nauk Fiz. Tekh. Nauki* **500** 7 (2021)
92. Wang X et al. *Appl. Phys. B* **124** 207 (2018)
93. Yu K, Ren J, Zhao Y *Artif. Intell. Agric.* **4** 127 (2020)
94. Soodan R K et al. *Talanta* **125** 405 (2014)
95. Palmer P T et al. *J. Agric. Food Chem.* **57** 2605 (2009)
96. Arantes de Carvalho G G et al. *J. Anal. Atom. Spectrom.* **33** 919 (2018)
97. Sdvizhenskii P A, Lednev V N *Phys. Wave Phenom.* **30** 37 (2022)
98. Lednev V N et al. *Phys. Wave Phenom.* **29** 221 (2021)
99. Yang Z et al. *Sensors* **22** 5858 (2022)
100. Senesi G S et al. *Environmental Res.* **109** 413 (2009)
101. Wisbrun R et al. *Anal. Chem.* **66** 2964 (1994)
102. Ciucci A et al. *Appl. Phys. B* **63** 185 (1996)
103. Popov A M et al. *Spectrochim. Acta B* **148** 205 (2018)
104. Pershin S M *Quantum Electron.* **39** 63 (2009); *Kvantovaya Elektron.* **39** 63 (2009)
105. Corsi M et al. *Appl. Geochem.* **21** 748 (2006)
106. Erler A et al. *Sensors* **20** 418 (2020)
107. Díaz D, Hahn D W, Molina A *Appl. Spectrosc.* **66** 99 (2012)
108. Zaytsev S M et al. *Spectrochim. Acta B* **140** 65 (2018)
109. Villas-Boas P R et al. *Geoderma* **263** 195 (2016)
110. Ferreira E C et al. *Spectrochim. Acta B* **110** 96 (2015)
111. Zhang Y, Zhang T, Li H *Spectrochim. Acta B* **181** 106218 (2021)

112. Sobral H, Sanginés R, Trujillo-Vázquez A *Spectrochim. Acta B* **78** 62 (2012)
113. Kang J et al. *J. Anal. Atom. Spectrom.* **32** 2292 (2017)
114. Järvinen S T, Saarela J, Toivonen J *Spectrochim. Acta B* **86** 55 (2013)
115. Sezer B, Bilge G, Boyaci I H *TrAC Trends Anal. Chem.* **97** 345 (2017)
116. Yang P et al. *J. Anal. Atom. Spectrom.* **37** 1948 (2022)
117. Lednev V N et al. *J. Anal. Atom. Spectrom.* **37** 2563 (2022)
118. Nunes L C et al. *J. Anal. Atom. Spectrom.* **25** 1453 (2010)
119. Barbafieri M et al. *Chem. Ecology* **27** (sup1) 161 (2011)
120. Galiová M et al. *Spectrochim. Acta B* **62** 1597 (2007)
121. Kaiser J et al. *Spectrochim. Acta B* **64** 67 (2009)
122. Kumar R et al. *Spectrosc. Lett.* **47** 554 (2014)
123. Krajcarová L et al. *Talanta* **173** 28 (2017)
124. Modlitbová P, Pořízka P, Kaiser J *TrAC Trends Anal. Chem.* **122** 115729 (2020)
125. Lednev V N et al. *Photonics* **8** 563 (2021)
126. Lednev V N et al. *Appl. Opt.* **62** 2030 (2023)
127. Bilge G et al. *Eur. Food Res. Technol.* **242** 1685 (2016)
128. Martelli M R et al. *J. Agric. Food Chem.* **58** 7126 (2010)
129. Zhao M et al. *Food Chem.* **309** 125704 (2020)
130. Moncayo S et al. *Talanta* **158** 185 (2016)
131. Andersen M-B S et al. *Food Control* **64** 226 (2016)
132. Kim G et al. *J. Agric. Food Chem.* **60** 718 (2012)
133. Jabbar A et al. *Optoelectron. Lett.* **15** 57 (2019)
134. Senesi G S, Harmon R S, Hark R R *Spectrochim. Acta B* **175** 106013 (2021)
135. Penkov N V, Penkova N A *Phys. Wave Phenom.* **29** 164 (2021)
136. Likhachev I G, Pustovoy V I *Phys. Wave Phenom.* **30** 91 (2022)
137. Berry G C *J. Solution Chem.* **25** 919 (1996)
138. Palberg T, Ballauff M (Eds) *Optical Methods and Physics of Colloidal Dispersions* (Progress in Colloid and Polymer Science, Vol. 104) (Berlin: Springer-Verlag, 1997) https://doi.org/10.1007/BFb0110733
139. Arwin H et al. *Appl. Sci.* **11** 6742 (2021)
140. Boulvert F et al. *Opt. Commun.* **282** 692 (2009)
141. Ignatenko D N et al. *Appl. Sci.* **12** 5258 (2022)
142. Shkirin A V et al. *Agriculture* **11** 1028 (2021)
143. Shkirin A V et al. *Phys. Wave Phenom.* **30** 186 (2022)
144. Kolokolova L et al. *J. Quant. Spectrosc. Radiat. Transf.* **100** 199 (2006)
145. Ghosh N, Vitkin A I *J. Biomed. Opt.* **16** 110801 (2011)
146. Fanjul-Velez F et al., in *2007 29th Annual Intern. Conf. of the IEEE Engineering in Medicine and Biology Society, 22–26 August 2007* (Piscataway, NJ: IEEE, 2007) p. 3339, https://doi.org/10.1109/IEMBS.2007.4353045
147. Ramella-Roman J C, Prahl S A, Jacques S L *Opt. Express* **13** 4420 (2005)
148. Ramella-Roman J C, Prahl S A, Jacques S L *Opt. Express* **13** 10392 (2005)
149. Wang X, Yao G, Wang L V *Appl. Opt.* **41** 792 (2002)
150. Wang L-F "Monte Carlo simulation model for electromagnetic scattering from vegetation and inversion of vegetation parameters," Thesis Ph.D. (Cambridge, MA: Massachusetts Institute of Technology, 2007); http://hdl.handle.net/1721.1/38923
151. Tuchin V V *J. Biomed. Opt.* **21** 071114 (2016) https://doi.org/10.1117/1.JBO.21.7.071114
152. Tuchin V V, Dan Z, Genina E A *Handbook of Tissue Optical Clearing: New Prospects in Optical Imaging* (Boca Raton, FL: CRC Press, 2022)
153. Shindo Y et al. *Rev. Sci. Instrum.* **64** 1161 (1993)
154. Protsenko E D, Tymper S I, Shkirin A V *Instrum. Exp. Tech.* **51** 268 (2008); *Prib. Tekh. Eksp.* (2) 118 (2008)
155. He H et al. *J. Lightwave Technol.* **37** 2534 (2019)
156. Pezzaniti J L, Chipman R A *Opt. Eng.* **34** 1558 (1995) https://doi.org/10.1117/12.202109
157. Mujat M, Ferguson R D, Iftimia N "Mueller matrix microscopy," in *Polarization Science and Remote Sensing VI, 26, 28–29 August 2013, San Diego, CA, USA* (Proc. SPIE, Vol. 8873, Eds J A Shaw, D A LeMaster) (Bellingham, WA: SPIE, 2013) p. 88730E
158. Chue-Sang J et al. *J. Biomed. Opt.* **21** 071109 (2016)
159. Lundblad J R, Laurance M, Goodman R H *Mol. Endocrinology* **10** 607 (1996) https://doi.org/10.1210/mend.10.6.8776720
160. Deibler L L, Smith M H *Appl. Opt.* **40** 3659 (2001)
161. Burmistrov D E et al. *Photonics* **8** 551 (2021)
162. Kalinin A V, Krasheninnikov V N *J. Appl. Spectrosc.* **75** 288 (2008)
163. Lei Y et al. *J. Mol. Struct.* **974** 88 (2010)
164. Cheruiyot E K et al. *Front. Genet.* **9** 607 (2018) https://doi.org/10.3389/fgene.2018.00607
165. Rienesl L et al. *Acta Univ. Agric. Silvic. Mendelianae Brun.* **67** 1221 (2019)
166. Khakimov A R et al. *Appl. Sci.* **12** 6621 (2022)
167. Balabin R M, Smirnov S V *Talanta* **85** 562 (2011) https://doi.org/10.1016/j.talanta.2011.04.026
168. Moguilnaia T Yu et al., in *Photonic Detection and Intervention Technologies for Safe Food* (Proc. SPIE, Vol. 4206, Eds Y-R Chen, S-I Tu) (Bellingham, WA: SPIE, 2000) p. 256
169. Cattaneo T M P, Holroyd S E *J. Near Infrared Spectrosc.* **21** 341 (2013)
170. Ageev A I, Osiptsov A N *Dokl. Phys.* **65** 242 (2020); *Dokl. Ross. Akad. Nauk Fiz. Tekh. Nauki* **493** 38 (2020)
171. Mohamed H et al. *Food Chem.* **334** 127436 (2021)
172. Melenteva A et al. *Food Chem.* **203** 190 (2016)
173. Soyeurt H et al. *J. Dairy Sci.* **94** 1657 (2011)
174. Shkirin A V et al. *Appl. Sci.* **12** 12517 (2022)
175. Kirsanov V V et al. *Photonics* **8** 390 (2021)
176. Khosroshahi M E, Patel Y, Woll-Morison V *Laser Phys. Lett.* **19** 075602 (2022)
177. Shcherbakov I A *Dokl. Phys.* **65** (6) 195 (2020); *Dokl. Ross. Akad. Nauk Fiz. Tekh. Nauki* **492** 4 (2020)
178. Nikitin E A et al. *Appl. Sci.* **12** 3230 (2022)
179. Belyakov M V, Nikitin E A, Efremenkov I Yu *Sel'skokhoz. Mashiny Tekhnol.* **16** (3) 55 (2022) https://doi.org/10.22314/2073-7599-2022-16-3-55-61
180. Belyakov M V et al. *Tekh. Oborudovanie Dlya Sela* (2) 31 (2023)
181. Lemire J A, Harrison J J, Turner R J *Nat. Rev. Microbiol.* **11** 371 (2013)
182. Gudkov S V et al. *Front. Phys.* **9** 641481 (2021)
183. Gudkov S V et al. *Pharmaceuticals* **15** 968 (2022)
184. Sondi I, Salopek-Sondi B *J. Colloid Interface Sci.* **275** 177 (2004)
185. Gomaa E Z *J. Gen. Appl. Microbiol.* **63** (1) 36 (2017)
186. Gabrielyan L et al. *Appl. Microbiol. Biotechnol.* **103** 2773 (2019)
187. Sullivan K T et al. *Combust. Flame* **160** 438 (2013)
188. Fenton H J H *J. Chem. Soc. Trans.* **65** 899 (1894)
189. Janani B et al. *J. Environment. Health Sci. Eng.* **19** 389 (2021)
190. Bruskov V I et al. *Free Radical Res.* **46** 1280 (2012)
191. Gudkov S V et al. *Nanomaterials* **12** 2635 (2022)
192. Das B et al. *Arabian J. Chem.* **10** 862 (2017)
193. Gudkov S V, Chernikov A V, Bruskov V I *Russ. J. Gen. Chem.* **86** 1531 (2016); *Ross. Khim. Zh.* **58** (3–4) 103 (2014)
194. Ocsoy I et al. *ACS Nano* **7** 8972 (2013)
195. AlMatar M et al. *Current Drug Deliv.* **15** 470 (2018)
196. Saha R K et al. *Sci. Rep.* **10** 2598 (2020)
197. Allahverdiyev A M et al. *Future Microbiol.* **6** 933 (2011)
198. Vernaya O I et al. *Moscow Univ. Chem. Bull.* **72** 6 (2017); *Vestn. Mosk. Univ. Ser. 2. Khim.* (6) 388 (2016)
199. Tyurikova I A et al. *ACS Omega* **5** 8146 (2020)
200. Lozhkomoev A S et al. *J. Nanopart. Res.* **23** 73 (2021)
201. Li W et al. *Biomater. Sci.* **8** 4492 (2020)
202. Pridvorova S M et al. *Phys. Wave Phenom.* **29** 47 (2021)
203. Luk'yanchuk B S et al. *Phys. Wave Phenom.* **30** 217 (2022)
204. Ashikkalieva K K et al. *Phys. Wave Phenom.* **30** 17 (2022)
205. Omelchenko A I et al. *Laser Phys.* **25** 025607 (2015)
206. Kostryukov V F, Igonina A E *Condens. Matter Interphases* **22** 504 (2020); *Kondens. Sredy Mezhfaznye Granitsy* **22** 504 (2020)
207. Abramova A V et al. *Beilstein J. Nanotechnol.* **5** 532 (2014)
208. Kazantsev S O et al. *Nanomaterials* **12** 3888 (2022)
209. Gudkov S V et al. *Antibiotics* **10** 884 (2021)
210. Smaoui S et al. *Food Packag. Shelf Life* **36** 101045 (2023)
211. Gudkov S V et al. *Int. J. Mol. Sci.* **24** 869 (2023)
212. Burmistrov D E et al. *Polymers* **14** 4764 (2022)
213. Simakin A V et al. *J. Compos. Sci.* **6** (10) 298 (2022)
214. Chausov D N et al. *Materials* **15** 527 (2022)
215. Tee B C-K et al. *Nat. Nanotechnol.* **7** 825 (2012)
216. Smirnova V V et al. *Materials* **14** 6915 (2021)
217. Tripathi S, Mehrotra G K, Dutta P K *Bull. Mater. Sci.* **34** 29 (2011)
218. Hu Z, Chan W L, Szeto Y S *J. Appl. Polymer Sci.* **108** 52 (2008)

219. Serov D A et al. *Nanomaterials* **12** 4158 (2022)
220. Serov D A et al. *Polymers* **14** 4880 (2022)
221. Ranieri P et al. *Plasma Process. Polym.* **18** 2000162 (2021)
222. Judickaité A et al. *Plants* **11** 611 (2022)
223. Mildaziene V, Sera B *Plants* **11** 1018 (2022)
224. Attri P et al. *Processes* **8** 1002 (2020)
225. Ohta T "Plasma in agriculture," in *Cold Plasma in Food and Agriculture. Fundamentals and Applications* (Eds N N Misra, O Schlüter, P J Cullen) (Amsterdam: Elsevier. Academic Press, 2016) p. 205, https://doi.org/10.1016/B978-0-12-801365-6.00008-1
226. Shcherbakov I A *Phys. Wave Phenom.* **30** 129 (2022)
227. Bunkin N F et al. *Phys. Wave Phenom.* **30** 196 (2022)
228. Pogorelov A G et al. *Phys. Wave Phenom.* **30** 209 (2022)
229. Shcherbakov I A *Phys. Wave Phenom.* **29** 89 (2021)
230. Bruskov V I et al. *Phys. Wave Phenom.* **29** 94 (2021)
231. Gudkov S V et al. *Phys. Wave Phenom.* **29** 108 (2021)
232. Svidlov A A et al. *Phys. Wave Phenom.* **29** 180 (2021)
233. Shutov D A et al. *Plasma Chem. Plasma Process.* **43** 577 (2023)
234. Piskarev I M *Plasma Chem. Plasma Process.* **41** 1347 (2021)
235. Sirotkin N A, Khlyustova A V, Titov V A *Plasma Chem. Plasma Process.* **40** 187 (2020)
236. Piskarev I M *Plasma Chem. Plasma Process.* **41** 1415 (2021)
237. Piskarev I M, Ivanova I P *Plasma Chem. Plasma Process.* **41** 447 (2021)
238. Bychkov V L et al. *IEEE Trans. Plasma Sci.* **49** 1034 (2021)
239. Bychkov V L et al. *IEEE Trans. Plasma Sci.* **48** 350 (2020)
240. Artem'ev K V et al. *Russ. Phys. J.* **62** 2073 (2020); *Izv. Vyssh. Uchebn. Zaved. Fiz.* (11) 105 (2019)
241. Konchekov E M et al. *Front. Phys.* **8** 616385 (2021)
242. Barkhudarov E M et al. *J. Atom. Mol. Phys.* **2013** 429189 (2013)
243. Naumova I K et al. *Priklad. Fiz.* (4) 40 (2021)
244. Belov S V et al. *Front. Phys.* **8** 618320 (2021)
245. Danileiko Y K et al. *Opera Med. Physiol.* **9** (3) 15 (2022)
246. Belov S V et al. *Processes* **10** 1536 (2022)
247. Danilejko Yu K et al. *Plants* **10** 2161 (2021)
248. Konchekov E M et al. *Plants* **11** 1373 (2022)
249. Kuzin A et al. *Plants* **12** 385 (2023)
250. Izmailov A et al. *Appl. Sci.* **12** 4953 (2022)
251. Astashev M E et al. *Sensors* **22** 8310 (2022)
252. Filippov R A et al. *Appl. Sci.* **13** 583 (2023)
253. Antipov S N et al. *Phys. Scr.* **98** 025604 (2023)
254. Antipov S N et al. *Plasma Phys. Rep.* **49** 559 (2023); *Fiz. Plazmy* **49** 407 (2023)
255. Sergeichev K F et al. *Front. Phys.* **8** 614684 (2021)
256. Ashurov M Kh et al. *ChemEngineering* **6** (6) 91 (2022)
257. Ali M M et al. *Physiol. Mol. Plant Pathol.* **108** 101426 (2019)
258. Farber C et al. *TrAC Trends Anal. Chem.* **118** 43 (2019)
259. Terentev A et al. *Sensors* **22** 757 (2022)
260. Dorokhov A et al. *Agriculture* **13** 1188 (2023)
261. Pankin D et al. *Agronomy* **11** 2402 (2021)
262. Moskovskiy M N et al. *Photonics* **8** 587 (2021)
263. Moskovskiy M N et al. *Agriculture* **13** 619 (2023)
264. Belyakov M V et al. *Appl. Sci.* **12** 4824 (2022)
265. Chen M et al. *Plos One* **17** (7) e0270593 (2022) https://doi.org/10.1371/journal.pone.0270593
266. Matveyeva T A et al. *Appl. Sci.* **12** 3391 (2022)
267. Sarimov R M et al. *Front. Phys.* **8** 640887 (2021)
268. Penkov N V et al. *Pathogens* **10** 1336 (2021)
269. Di Girolamo F V et al. *Food Control* **123** 107700 (2021)
270. Ge H et al. *Photonics* **8** 518 (2021)